

NBS-GCR-84-481

**PRACTICAL APPROXIMATIONS OF PEAK
WAVE FORCES**

Mircea Grigoriu and Bunu Alibe

School of Civil and Environmental Engineering
Cornell University
Hollister Hall
Ithaca, NY 14853

November 1984

Prepared for
Minerals Management Service
Reston, VA 22091

FOREWORD

The Technology Assessment and Research Branch of the Minerals Management Service (MMS), United States Department of the Interior, is engaged in a program of research and development to provide information on the performance of offshore systems. As part of this program, MMS is sponsoring the project "Assessment of Uncertainties and Risks Associated with the Dynamic Behavior of Compliant Structures" under contract with the National Bureau of Standards (NBS).

Among these uncertainties and risks are those related to the effects of currents and waves. The purpose of this report is to apply recent developments in the theory of extremes of random processes to the estimation of peak wave forces that may be described by the Morison equation. Descriptors of wave forces -- which are non-Gaussian -- are provided that are useful in reliability calculations, e.g., mean crossing rates and extreme value distributions. An approximate procedure for estimating peak wave forces is presented that is simple and convenient for practical use, and that is applicable regardless of the magnitude of the current and of the ratio between the inertia and the drag component of the wave force.

Emil Simiu
Structures Division
Center for Building Technology
National Bureau of Standards

ABSTRACT

According to Morison's equation, wave forces acting on cylindrical members have two components: drag forces, which depend nonlinearly on wave particle velocity, and inertia forces, which are proportional to wave particle acceleration. Wave forces are then non-Gaussian processes although fluid velocities are assumed to follow Gaussian distributions. This report develops approximations of the mean of the peak of wave forces during design storms. It shows that the square root of the sum of the squares (SRSS) rule can be applied to approximate the mean of the peak wave force from the average peaks of inertia and drag forces. The approximation is satisfactory for any ratio of drag to inertia forces and frequency content of the wave particle velocity process. The report also provides various descriptors of drag, inertia, and wave forces, including marginal distributions, mean crossing rates, and extreme value distributions.

DISCLAIMER

The statements and conclusion contained in this report are those of the contractor and do not necessarily reflect the view of the U.S. Government and, in particular, the National Bureau of Standards or the Department of the Interior. Neither NBS or the contractors make any warranty, express or implied, or assume any legal liability or responsibility for the accuracy, completeness or usefulness of any information, apparatus, product or process disclosed or represent that its use would not infringe privately owned rights. They accept no responsibility for any damage that may result from the use of any information contained herein. The mentioning of manufacturers, professional firms, names, products, and the publication of performance data do not constitute any evaluation or endorsement by the U.S. Government, its agencies, or the contractor. It is done in a generic sense to illustrate particular points.

PRACTICAL APPROXIMATIONS OF PEAK WAVE FORCES

By Mircea Grigoriu and Bunu Alibe

INTRODUCTION

According to Morison's equation, wave forces acting on cylindrical members have two components: drag forces, which depend nonlinearly on wave particle velocity, and inertia forces, which are proportional to wave particle acceleration (1). Wave forces are then non-Gaussian processes although fluid velocities are assumed to follow Gaussian distributions.

This report develops approximations of the mean of the peak of wave forces during design storms. It shows that the square root of the sum of the squares (SRSS) rule can be applied to approximate the mean of the peak wave force from the average peaks of inertia and drag forces. The approximation is satisfactory for any ratio of drag to inertia forces and frequency content of the wave particle velocity process. As shown in Appendix A, previous studies have rarely considered the joint action of inertia and drag forces and have generally examined characteristics of drag forces with small or zero current. Appendix A provides also additional descriptors of drag, inertia, and wave forces, e.g., marginal distributions, mean crossing rates, and extreme value distributions. These descriptors were used in the report to test various approximations. However, the report and Appendix A can be read independently.

WAVE FORCES

Let $Y^*(t)$ be the wave particle velocity at any time t . It is assumed that $Y^*(t)$ is a twice-differentiable, stationary Gaussian process with positive mean y_0 , variance σ_Y^2 , and autocovariance function $B_Y(\tau) = \sigma_Y^2 \rho_Y(\tau)$. The process will be viewed in the analysis as the sum of two components, the current, y_0 , and the zero-mean fluctuating component, $Y(t)$,

$$Y^*(t) = y_0 + Y(t) \quad (1)$$

The variances of $\dot{Y}(t) = dY(t)/dt$ and $Y(t) = d^2Y(t)/dt^2$, which are needed to characterize inertia forces, can be determined from the following expressions (2)

$$\sigma_{\dot{Y}}^2 = - \alpha_Y^2 \frac{d^2}{d\tau^2} \rho_Y(\tau) \Big|_{\tau=0} \quad (2)$$
$$\sigma_{Y''}^2 = \alpha_Y^2 \frac{d^4}{d\tau^4} \rho_Y(\tau) \Big|_{\tau=0}$$

According to Morison's equation (1), wave forces are proportional to

$$R(t) = X_1(t) + X_2(t) \quad (3)$$

in which the process

$$X_1(t) = (y_0 + Y(t)) \Big| y_0 + Y(t) \Big| \quad (4)$$

denotes drag forces and

$$X_2(t) = a \dot{Y}(t) \quad (5)$$

characterizes inertia forces. The coefficient a is a measure of the relative importance of inertia forces with respect to drag forces, e.g., inertia forces are negligible for small values of a .

The relative magnitude of the components of wave forces can be evaluated in terms of the parameters

$$\alpha = \frac{\sigma_Y}{y_0}$$

$$\beta = \frac{a\sigma_{\dot{Y}}}{y_0^2} \tag{6}$$

$$\delta = \frac{\sigma_{\ddot{Y}} a}{\sigma_{\dot{Y}} y_0}$$

For example, there is no current when α becomes infinity. The parameter β quantifies the importance of inertia forces with respect to drag forces (e.g., small values of β indicate dominant drag forces). δ is a derived parameter which, as β , depends on the power spectral density function of $Y(t)$. Table 1 gives values of β and δ for a Pierson-Moskowitz spectrum with wind velocity of $V = 20$ knots and a cutoff frequency of 3.5 rad/sec. It is assumed, as in Ref. 6, that the current y_0 takes on values in the interval $(1/50, 1/20)$ v. Resultant range of values for α is $1 \leq \alpha \leq 20$.

AVERAGE PEAK OF RANDOM PROCESSES

Consider a differentiable random process, $X(t)$, with mean m and variance σ^2 . Let σ^2 be the variance of $\dot{X}(t) = dX(t)/dt$. This section provides approximations for the average of the peak of $X(t)$ during any period τ , i.e., the function

$$m_\tau = E \left[\max_{\tau} \{X(t)\} \right] \tag{7}$$

Gaussian Processes

It can be shown that m_τ can be approximated by

$$\bar{m}_\tau = m + \sigma \left[\sqrt{2 \ln v_0 \tau} + \frac{\gamma}{\sqrt{2 \ln v_0 \tau}} \right] \quad (8)$$

when $X(t)$ is a Gaussian process (3). In this approximation $\gamma = 0.577216 =$ the Euler's constant and

$$v_0 = \frac{1}{2\pi} \frac{\dot{\sigma}}{\sigma} \quad (9)$$

is the mean zero-crossing rate.

The approximation in Eq. 8 is satisfactory in many cases but fails when applied to narrow-band processes. For example, assume that $X(t)$ is a monochromatic process, i.e., a sinusoidal wave with random phase and amplitude. The peak of any sample $X(t)$ is equal to the corresponding realization of the amplitude and does not depend on the observation period τ , provided that τ exceeds the period of the wave. Thus, m_τ is the average of the amplitude of the wave for any τ . On the other hand, \bar{m}_τ in Eq. 8 is an increasing function of this parameter.

Figure 1 shows the dependence of m_τ and \bar{m}_τ on $v_0 \tau$ for a zero-mean, unit-variance Gaussian process $X(t)$ with various bandwidth parameters, q . The bandwidth parameter q is (5)

$$q = \sqrt{1 - \frac{\lambda_1^2}{\lambda_0 \lambda_2}} \quad (10)$$

in which

$$\lambda_i = \int_0^{\infty} \omega^i G(\omega) d\omega \quad (11)$$

and $G(\omega)$ denotes the power spectral density of $X(t)$. It is zero for monochromatic processes and approaches unity as the bandwidth of $X(t)$ increases. Note that there are significant differences between m_τ and \tilde{m}_τ , particularly for small values of q (i.e., when $X(t)$ is a narrow-band process). However, \tilde{m}_τ constitutes a satisfactory approximation of m_τ for $q \geq 0.1$. The exact value m_τ was obtained by numerical integration from the largest value distribution of the process $X(t)$ in τ , which is available in the literature (2).

The approximation in Eq. 8 can be improved if v_0 is decreased to account for the dependence between the peaks of $X(t)$, which can be strong for narrow-band processes (5). Figure 2 shows the variation of m_τ and the approximation

$$\tilde{m}_\tau^* = m + \sigma \left(\sqrt{2 \ln v_0^* \tau} + \frac{\gamma}{\sqrt{2 \ln v_0^* \tau}} \right) \quad (12)$$

with $v_0^* \tau$ and q . This new approximation is similar to the one in Eq. 8 but uses the reduced value of the mean zero-crossing rate

$$v_0^* = v_0 (1 - e^{-3.5q}) \quad (13)$$

which was obtained empirically from results in Fig. 1. The approximations \tilde{m}_τ and \tilde{m}_τ^* in Eqs. 8 and 12 are nearly equal for $q \geq 0.1$, but differ significantly for smaller values of q . While the approximation in Eq. 8 is inaccurate for narrow-band processes, the latter approximation is satisfactory for any spectral characteristics of $X(t)$.

Non-Gaussian Processes

Let

$$X(t) = g(Y^*(t)) \tag{14}$$

in which $Y^*(t)$ is the Gaussian process in Eq. 1 and g denotes a monotonically increasing function. If the function g is nonlinear, $X(t)$ is a non-Gaussian process. The drag force is such a non-Gaussian process. In this case $g(Y^*(t)) = Y^*(t) | Y^*(t) |$. Note that $\max_{\tau} \{X(t)\}$ and $g(\max_{\tau} \{Y^*(t)\})$ are equal for any sample of $Y^*(t)$. However, $m_{\tau} = E[\max_{\tau} \{X(t)\}]$ is generally different from $g(E[\max_{\tau} \{Y^*(t)\}])$.

It can be shown that m_{τ} can be approximated by

$$\tilde{m}_{\tau,g} = g(y^*) + \frac{\gamma \sigma_Y g'(y^*)}{\sqrt{2 \ln v_{0,Y} \tau}} \tag{15}$$

in which

$$y^* = y_0 + \sigma_Y \sqrt{2 \ln v_{0,Y} \tau} \tag{16}$$

$$v_{0,Y} = \frac{1}{2\pi} \frac{\sigma_Y^2}{\sigma_Y}$$

The derivation of Eq. 15 is not given in this report because it involves elementary but lengthy calculations which are similar to those leading to Eq. 8. The approximation $\tilde{m}_{\tau,g}$ can be refined based on considerations as in Eq. 12.

PEAK DRAG FORCE

The mean of the peak drag force during storms of duration τ

$$m_{1,\tau} = E \left[\max_{\tau} \{X_1(t)\} \right] \quad (17)$$

is approximated by two methods.

First Method of Approximation

It has been suggested in practice to approximate $m_{1,\tau}$ by the value of the drag force corresponding to the average peak of the fluctuating component $Y(t)$, i.e., $g(E \left[\max_{\tau} \{Y^*(t)\} \right])$ in which $g(z) = z \left| z \right|$. The approximation can be given in the form

$$\tilde{m}_{1,\tau}^{(1)} = y_0^2 \left[1 + \alpha \left(\sqrt{2 \ln v_0 \tau} + \frac{\gamma}{\sqrt{2 \ln v_0 \tau}} \right) \right]^2 \quad (18)$$

for positive currents.

Table 2 gives exact and approximate average peaks of the drag force for selected values of $v_0 \tau$ and α . In all cases considered in the table, the approximation in Eq. 18 is slightly conservative. The approximation $\tilde{m}_{1,\tau}^{(2)}$ in the next section (Eq. 19) is also accurate but unconservative. The exact average peak of $X_1(t)$ was obtained by numerical integration based on developments in Appendix A.

Second Method of Approximation

According to Eq. 15, the mean of peak drag force can also be approximated by

$$\tilde{m}_{1,\tau}^{(2)} = y_0^2 \left[\left(1 + \alpha \sqrt{2 \ln v_0 \tau} \right)^2 + \frac{\gamma \alpha}{\sqrt{2 \ln v_0 \tau}} \left(1 + \alpha \sqrt{2 \ln v_0 \tau} \right) \right] \quad (19)$$

when the current is positive.

Table 3 gives ratios between the approximations in Eqs. 18 and 19 for selected values of $v_0\tau$ and α . Note that the differences between these approximations are generally minor and $\tilde{m}_{1,\tau}^{(2)}$ is smaller than $\tilde{m}_{1,\tau}^{(1)}$ in all cases considered. The largest difference between $\tilde{m}_{1,\tau}^{(1)}$ and $\tilde{m}_{1,\tau}^{(2)}$ occurs at $\alpha = \infty$ (the case of no current). The approximations coincide when $\alpha = 0$ (the case of a deterministic current and no fluctuating component).

It is of interest to examine characteristics of the average peaks of drag forces and wave particle velocities. Table 4 gives the averages of $\max_{\tau} \{Y^*(t)\}$ and $\max_{\tau} \{X_1(t)\}$ expressed as numbers of standard deviations of $Y^*(t)$ and $X_1(t)$, respectively, above the corresponding means. These numbers are k_y for $Y^*(t)$ and $k_x^{(1)}$ and $k_x^{(2)}$ for $X_1(t)$. They are based on the approximations in Eqs. 8, 18, and 19. Note that $k_x^{(1)}$ and $k_x^{(2)}$ are generally much larger than k_y . These differences are caused by the skewness in the distribution of $X_1(t)$. They decrease with y_0 because $X_1(t)$ has a less skewed distribution for large currents.

PEAK WAVE FORCES

Approximations are developed for the expectation

$$m_{R,\tau} = E \left[\max_{\tau} \{R(t)\} \right] \quad (20)$$

of the peak of the wave force $R(t)$ in a storm of duration τ . From Eq. 3, $R(t)$ is the sum of two random processes, $X_1(t)$ and $X_2(t)$, which are independent at any time t . Since characteristics of $R(t)$, such as mean zero-crossing rate,

mean, and variance, generally involve lengthy calculations, $m_{R,\tau}$ cannot be estimated simply from the approximations in the previous section. Other methods are then needed to find $m_{R,\tau}$.

It is proposed to approximate $m_{R,\tau}$ from the average peaks of the drag and the inertia forces, $m_{1,\tau}$ and $m_{2,\tau}$, based on rules used in structural dynamics for combinations of modal responses (4). According to these rules, $m_{R,\tau}$ can be approximated by

$$m_{ABS} = m_{1,\tau} + m_{2,\tau} \quad (21)$$

or

$$m_{SRSS} = \sqrt{m_{1,\tau}^2 + m_{2,\tau}^2} \quad (22)$$

These approximations are the so-called the absolute sum rule (ABS) and the square root of the sum of the squares rule (SRSS). It can be shown that the SRSS rule is superior for uncorrelated modal responses (4). Since $X_1(t)$ and $X_2(t)$ are independent at any t , it is expected that the SRSS be an accurate approximation of $m_{R,\tau}$. Note also that the averages $m_{1,\tau}$ and $m_{2,\tau}$ in Eqs. 21 and 22 can be replaced in practice by any of the approximations considered in the previous sections.

Figures 3, 4, and 5 show the variation of $m_{R,\tau}$, m_{ABS} , and m_{SRSS} with $v_0 \tau$ for wave particle velocity processes with narrow-band ($q = 0.1$), wide-band, and Pierson-Moskowitz spectra ($v = 20$ knots). The peak averages, $m_{1,\tau}$ and $m_{2,\tau}$, of the drag and inertia forces are approximated from Eq. 18 or 19 and Eq. 8 while $m_{R,\tau}$ was determined "exactly" by simulation. From Fig. 3 (a, b, c), the SRSS

rule is conservative for narrow-band wave particle velocities with $q = 0.1$, $\beta = 10$, and values of α corresponding to large, intermediate, and low currents (Table 1) when based on Eq. 18. Superior approximations result when the analysis is based on Eq. 19 which accounts specifically for the bandwidth of the process, see Fig. 3(d,e,f). The SRSS rule is also satisfactory when wave particle velocities are characterized by wide-band and Pierson-Moskowitz spectra (Figs. 4 and 5). The use of Eq. 19, instead of Eq. 18, does not improve the approximation in these cases because the bandwidth parameter, q , is relatively large. Figures 3 to 5 were developed for $\beta = 10$ because drag and inertia forces have similar magnitudes for this value of β . When these forces differ significantly, the ABS and SRSS rules practically coincide and the peak wave force can be approximated from either the drag or the inertia force and Eq. 8, 9, 18, or 19.

CONCLUSIONS

Simple approximations were proposed for the average peak of drag forces, inertia forces, and wave forces. The approximations involve elementary calculations and can account for the bandwidth of the wave particle velocity process. It was found that the SRSS rule can be applied to approximate the average peak of wave forces from the average peaks of inertia and drag forces.

REFERENCES

1. Borgman, L. E., "Statistical Models for Ocean Waves and Wave Forces," Advances in Hydroscience, Vol. 8, 1972, pp. 139-181.
2. Cramer, H. and Leadbetter, M. R., Stationary and Related Stochastic Processes, John Wiley & Sons, New York, 1967.
3. Davenport, A. G., "On the Statistical Prediction of Structural Performance in Wind Environment," presented at the April 19-23, 1971, ASCE National Structural Meeting, held at Baltimore, Maryland (Preprint 1420).

4. Grigoriu, M., "New Criteria for Selecting Modal Combination Rules," presented at the July 7-11, 1980, International Conference on Recent Advances in Structural Analysis, held at Southampton, England.
5. Vanmarcke, E. H., "On the Distribution of the First-Passage Time for Normal Stationary Random Processes," Journal of Applied Mechanics, TRANS. ASME, Vol. 42, No. 1, Series E, March, 1975, pp. 215-220.
6. Wiegel, R. L., "Ocean Dynamics," Hydrodynamics, ed. Sheets, H. E. and Boatwright, V. T., Jr., Academic Press, 1970.

TABLE 1 Wave Force Parameter δ

		$\alpha = 20$ (small current)	$\alpha = 2$ (intermediate current)	$\alpha = 1$ (large current)
β	.1	.0069	.0687	.1374
	.5	.0344	.3436	.6871
	1.0	.0687	.687	1.3742
	10.	0.6879	6.8700	13.7620
	100.	0.8700	68.7000	137.4200

TABLE 2 Comparisons Between Approximate and Exact Means of Peak Deag Forces

$v_0 \tau$	$\alpha = 20.$ (small current)			$\alpha = 2.$ (intermediate current)			$\alpha = 1.0$ (large current)		
	$\frac{m_{1,\tau}}{y_0^2}$	$\frac{\tilde{m}_{1,\tau}^{(1)}}{y_0^2}$	$\frac{\tilde{m}_{1,\tau}^{(2)}}{y_0^2}$	$\frac{m_{1,\tau}}{y_0^2}$	$\frac{\tilde{m}_{1,\tau}^{(1)}}{y_0^2}$	$\frac{\tilde{m}_{1,\tau}^{(2)}}{y_0^2}$	$\frac{m_{1,\tau}}{y_0^2}$	$\frac{\tilde{m}_{1,\tau}^{(1)}}{y_0^2}$	$\frac{\tilde{m}_{1,\tau}^{(2)}}{y_0^2}$
100	4270.	4290.	4041.	55.3	55.5	56.7	17.8	17.9	17.1
1000	6143.	6153.	5910.	76.3	76.5	73.8	23.7	23.7	23.0
5000	7466.	7455.	7213.	90.8	90.9	88.2	27.7	27.7	27.0
10000	8007.	8015.	7775.	97.0	97.1	94.4	29.4	29.5	28.7
50000	9309.	9316.	9075.	111.2	111.3	108.7	33.3	33.4	32.6
100000	9870.	9875.	9636.	117.4	117.5	114.9	35.0	35.0	34.3

TABLE 3 Ratios of $\tilde{m}_{1,\tau}^{(1)}$ and $\tilde{m}_{1,\tau}^{(2)}$

$v_0 \tau$	$\alpha = .1$	$\alpha = .5$	$\alpha = 1.0$	$\alpha = 2.0$	$\alpha = 4.0$	$\alpha = 20.$
100	1.0146	1.0378	1.0471	1.0538	1.0579	1.0617
1000	1.0113	1.0272	1.0329	1.0368	1.0391	1.0412
5000	1.0099	1.0228	1.0273	1.0302	1.0320	1.0335
10000	1.0094	1.0214	1.0254	1.0281	1.0296	1.0310
50000	1.0084	1.0187	1.0220	1.0241	1.0253	1.0264
100000	1.0089	1.0172	1.0207	1.0227	1.0238	1.0248

TABLE 4 Averages of Peak Wave Particle Velocities and Peak Drag Forces

$v_0 \tau$	$\alpha = 20.$ (small current)			$\alpha = 2.0$ (intermediate current)			$\alpha = 1.0$ (large current)		
	k_y	$k_x^{(1)}$	$k_x^{(2)}$	k_y	$k_x^{(1)}$	$k_x^{(2)}$	k_y	$k_x^{(1)}$	$k_x^{(2)}$
100	3.23	8.69	8.16	3.23	7.42	7.01	3.23	6.42	6.09
1000	3.87	12.66	12.14	3.87	10.44	10.05	3.87	8.79	6.48
5000	4.27	15.44	14.92	4.27	12.53	12.14	4.27	10.40	10.11
10000	4.43	16.63	16.12	4.43	13.42	13.04	4.43	11.09	10.79
50000	4.78	19.40	18.89	4.78	15.48	15.10	4.78	12.67	12.38
100000	4.92	20.60	20.09	4.92	16.36	15.99	4.92	13.34	13.05

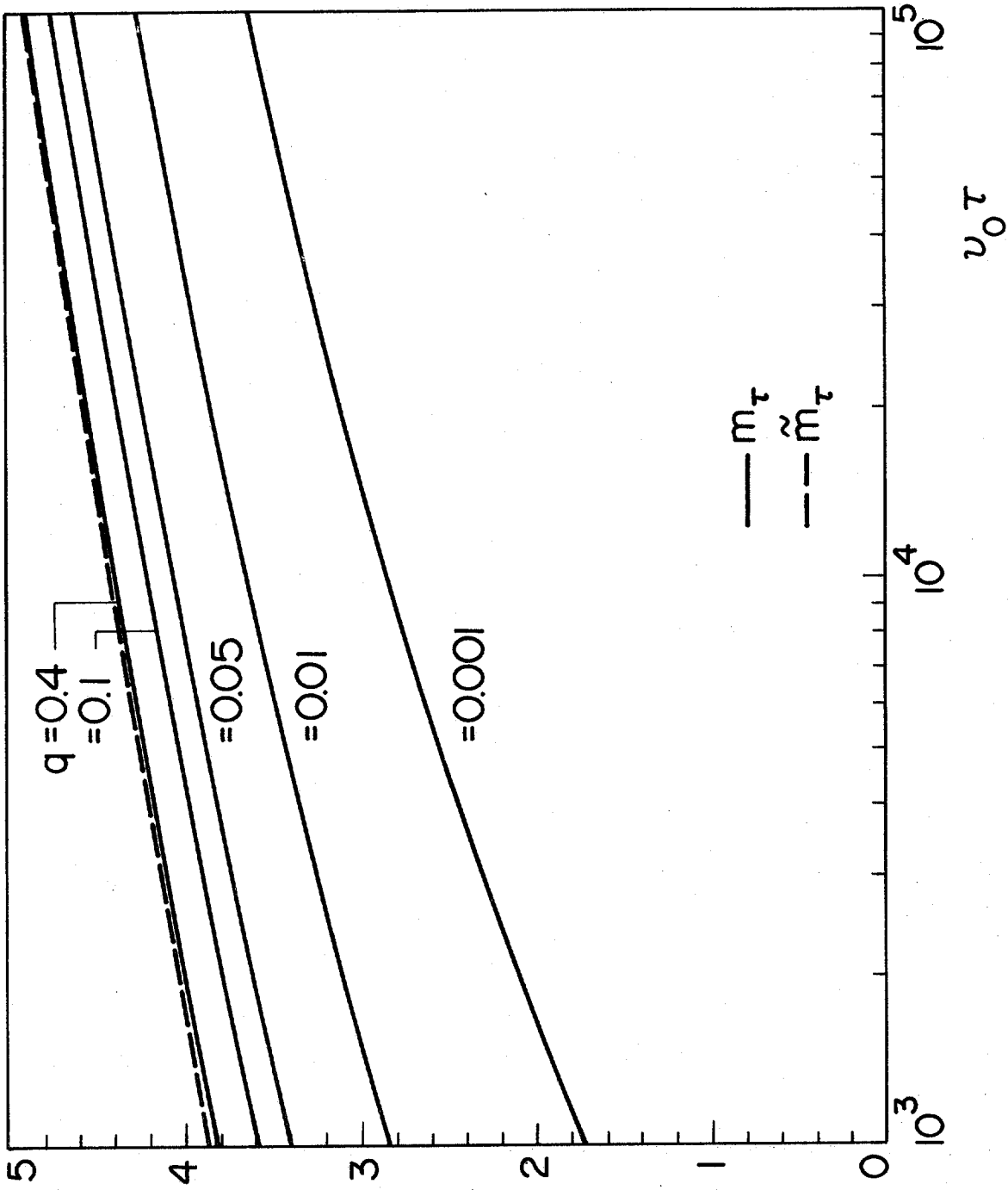


Figure 1. Mean of Peak of Gaussian Processes with Various Bandwidths ($m = 0, \sigma = 1.0$)

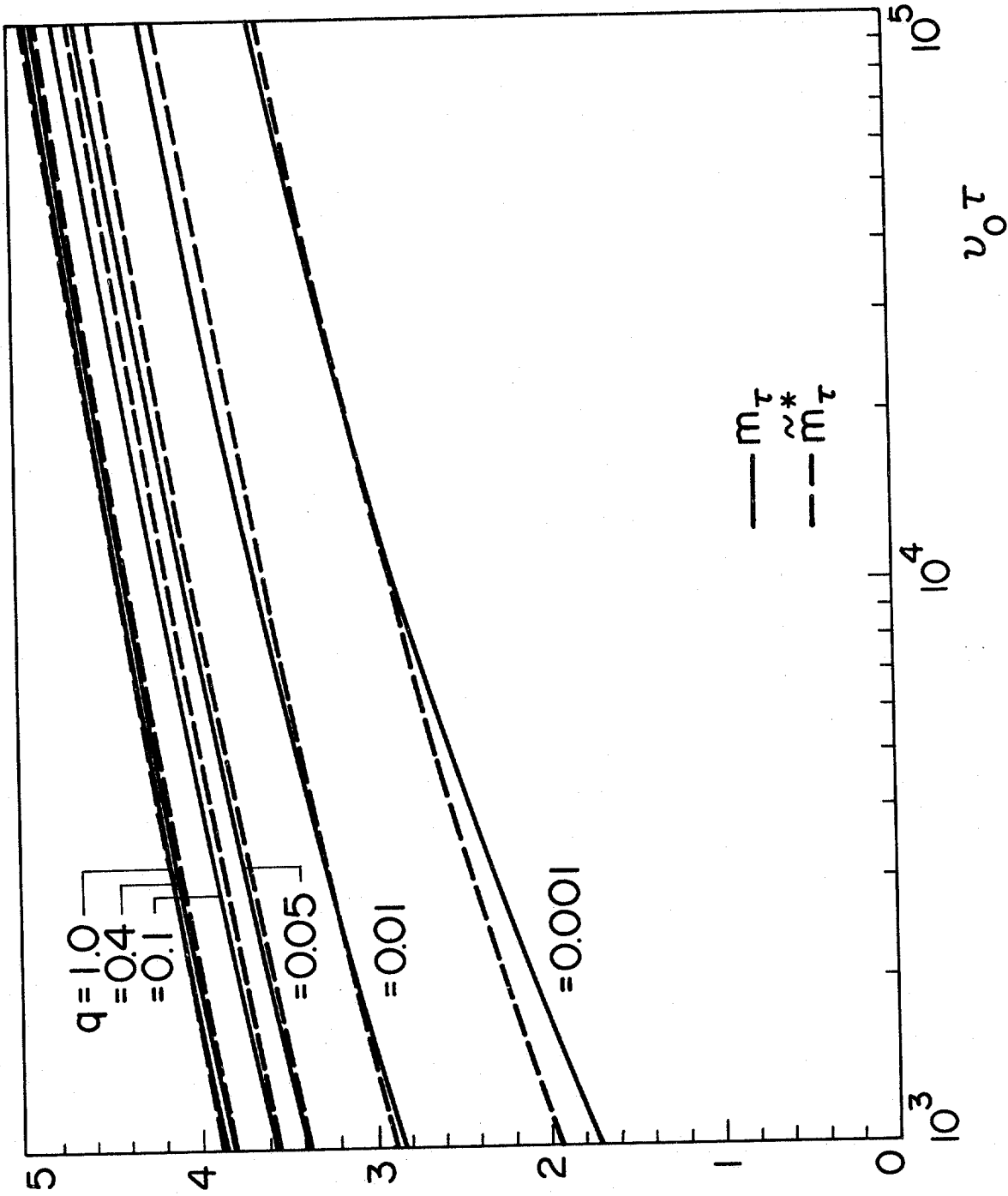
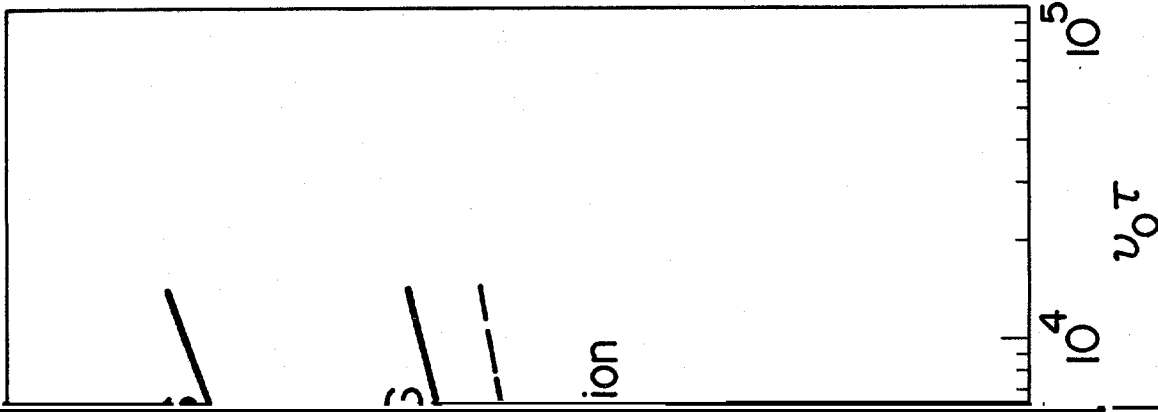


Figure 2. Exact and Approximate Means of Peak of Gaussian Processes with Various Bandwidths ($m = 0, \sigma = 1.0$)



re Forces
, $\beta = 10$,

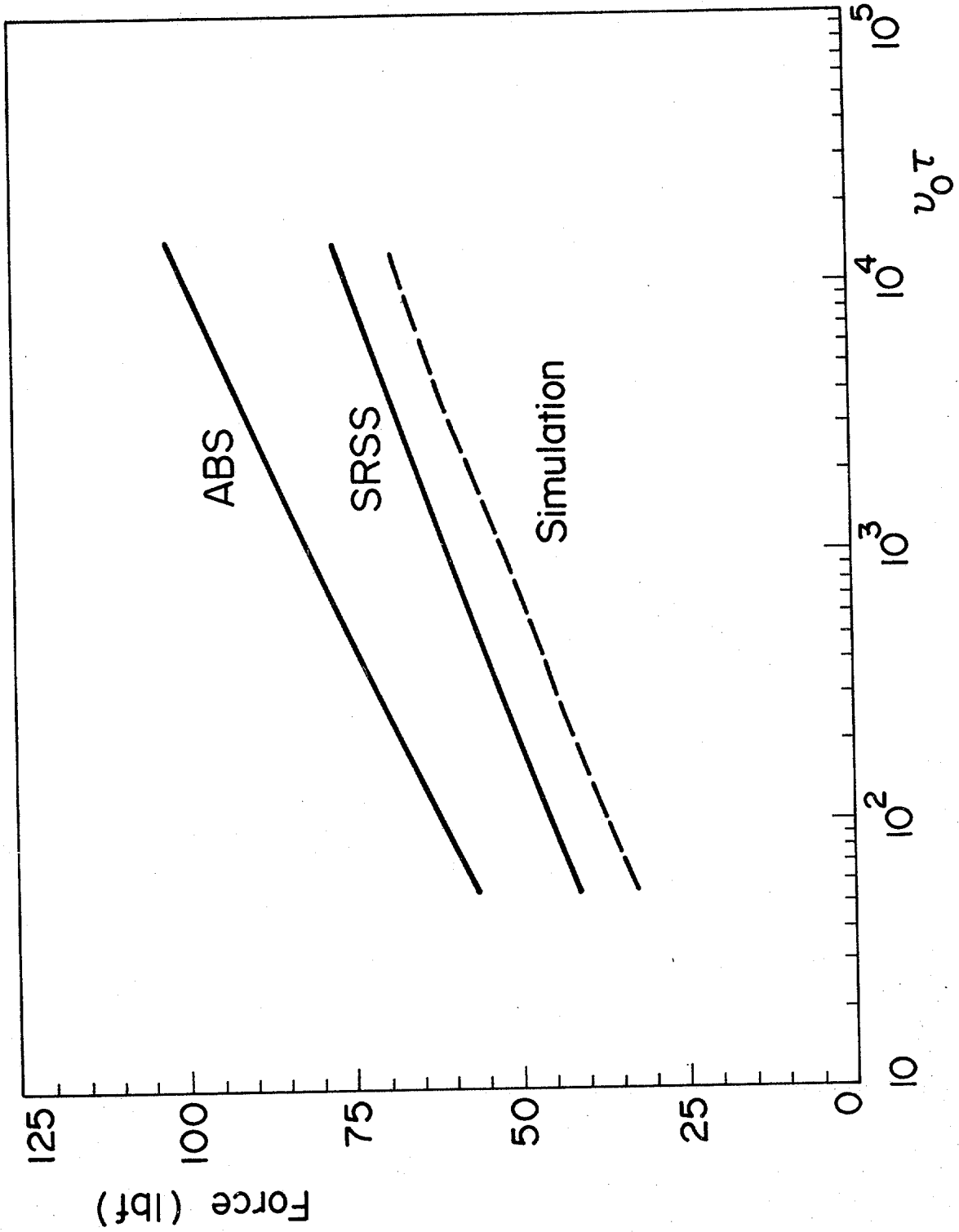


Figure 3(b). Exact and Approximate Means of Peak Wave Forces (Narrow-Band Wave Spectrum with $q = 0.1$, $\beta = 10$, and $\alpha = 2$)

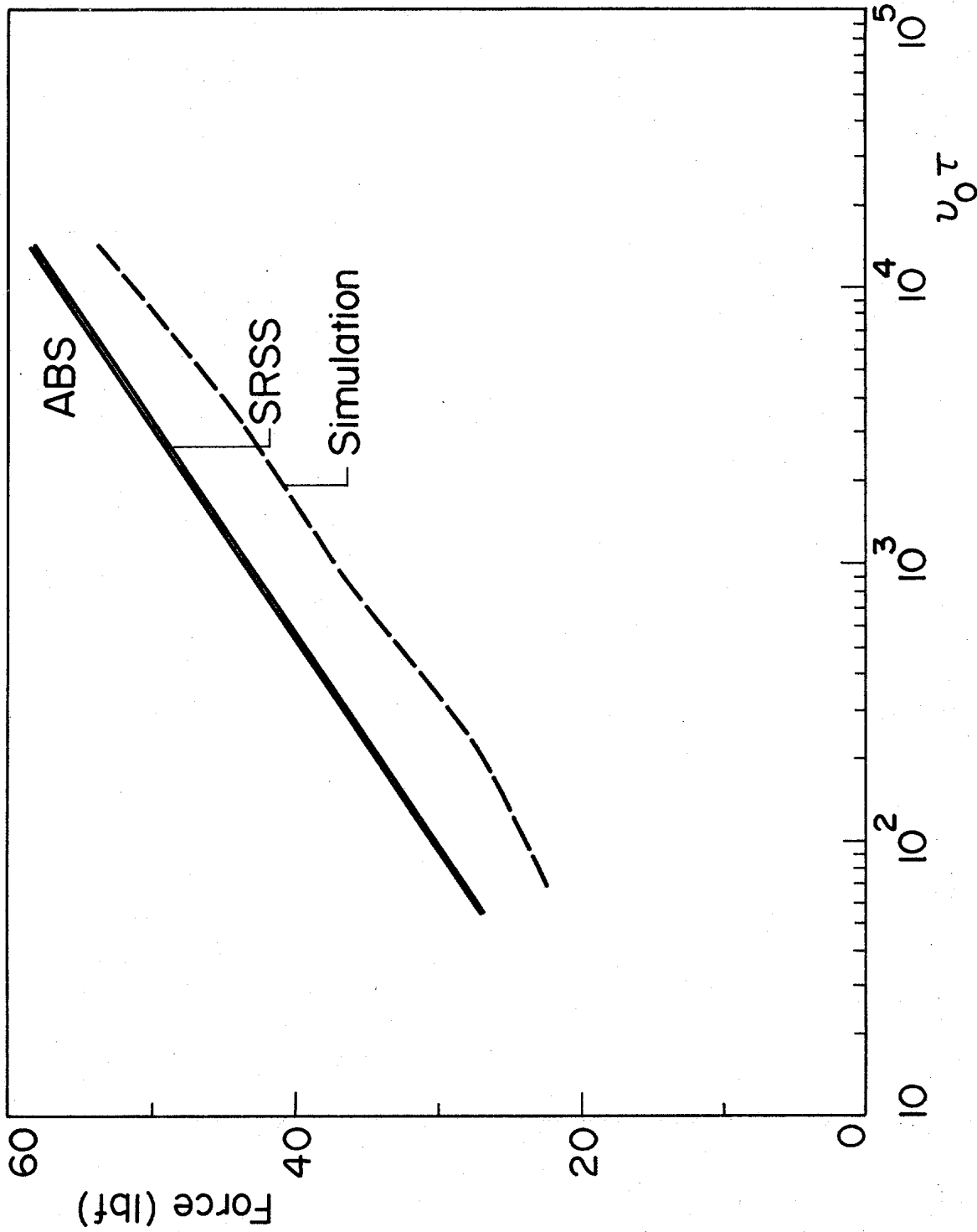


Figure 3(c). Exact and Approximate Means of Peak Wave Forces (Narrow-Band Wave Spectrum with $q = 0.1$, $\beta = 10$, and $\alpha = 20$)

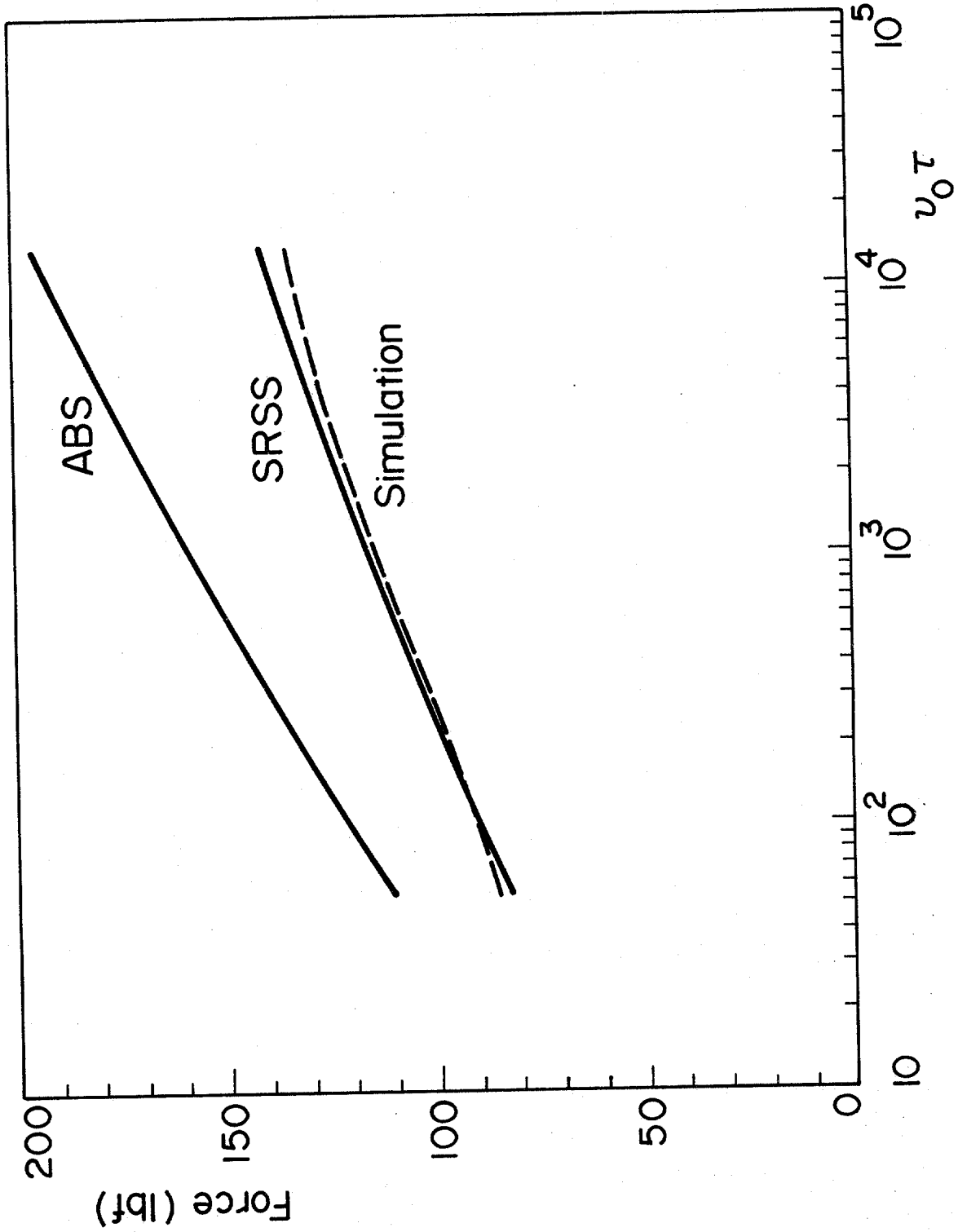


Figure 3(d). Exact and Approximate Means of Peak Wave Forces (Narrow-Band Wave Spectrum with $q = 0.1$, $\beta = 10$, and $\alpha = 1$)

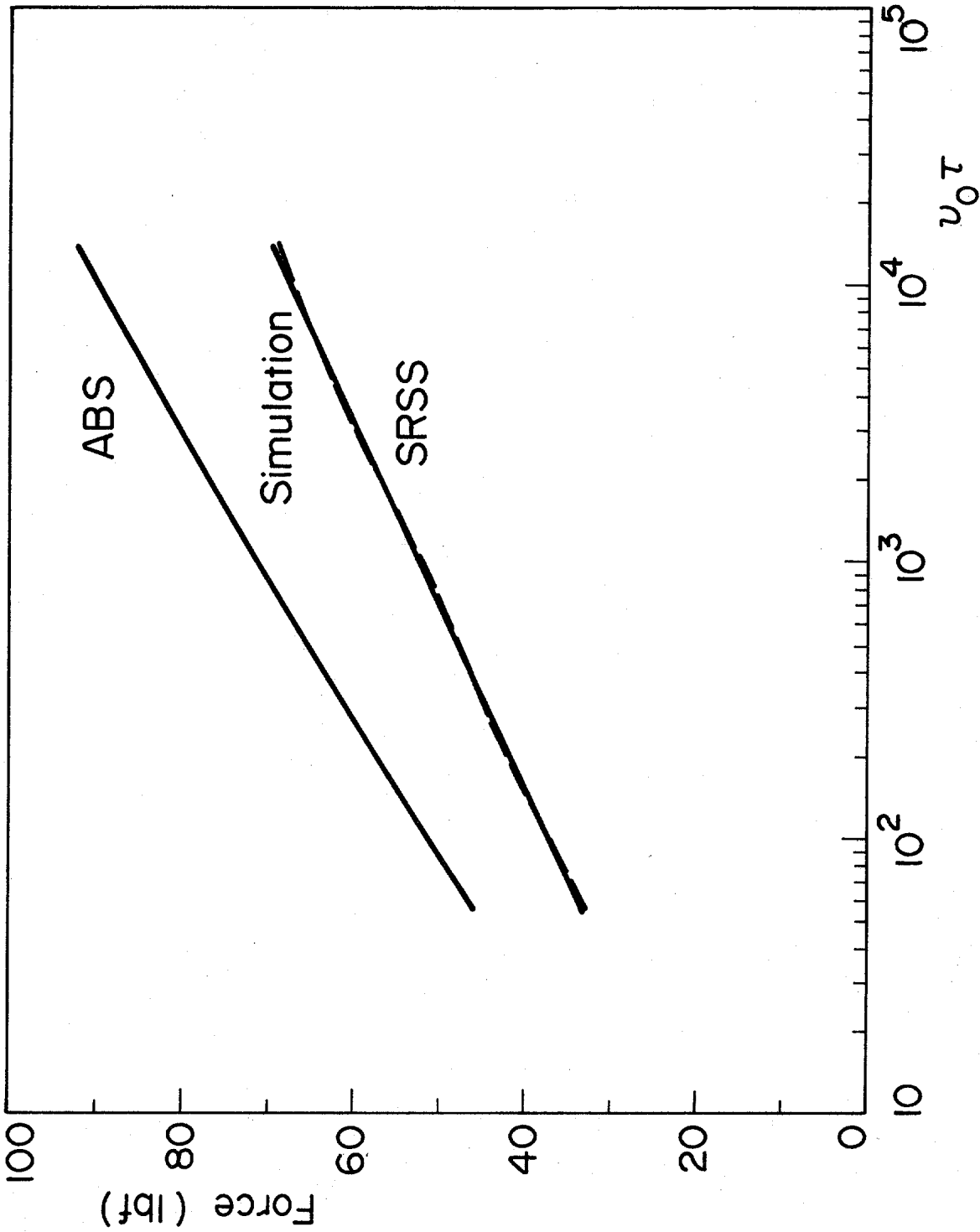


Figure 3(e). Exact and Approximate Means of Peak Wave Forces (Narrow-Band Wave Spectrum with $q = 0.1$, $\beta = 10$, and $\alpha = 2$)

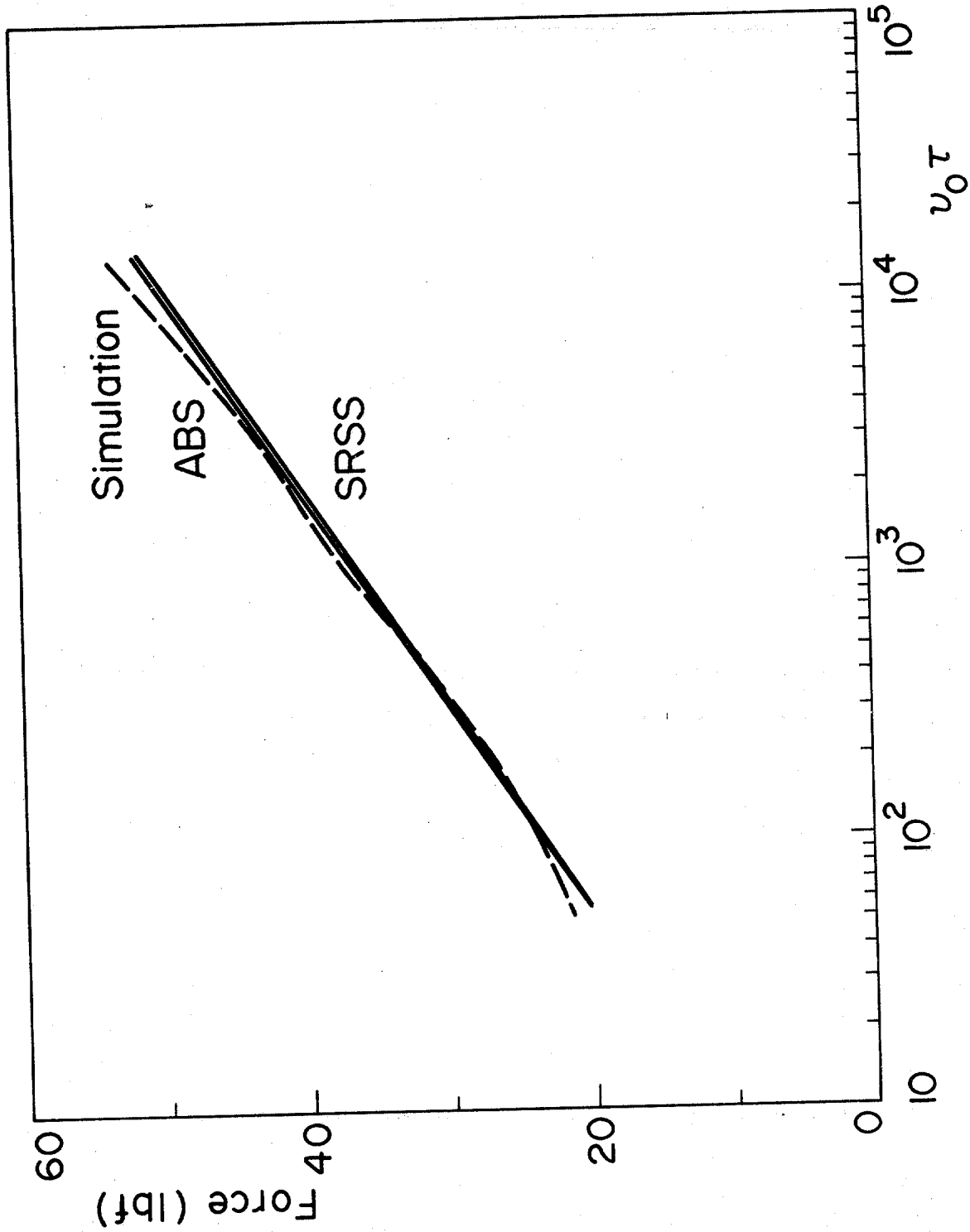


Figure 3(f). Exact and Approximate Means of Peak Wave Forces
(Narrow-Band Wave Spectrum with $q = 0.1$, $\beta = 10$,
 $\alpha = 20$)

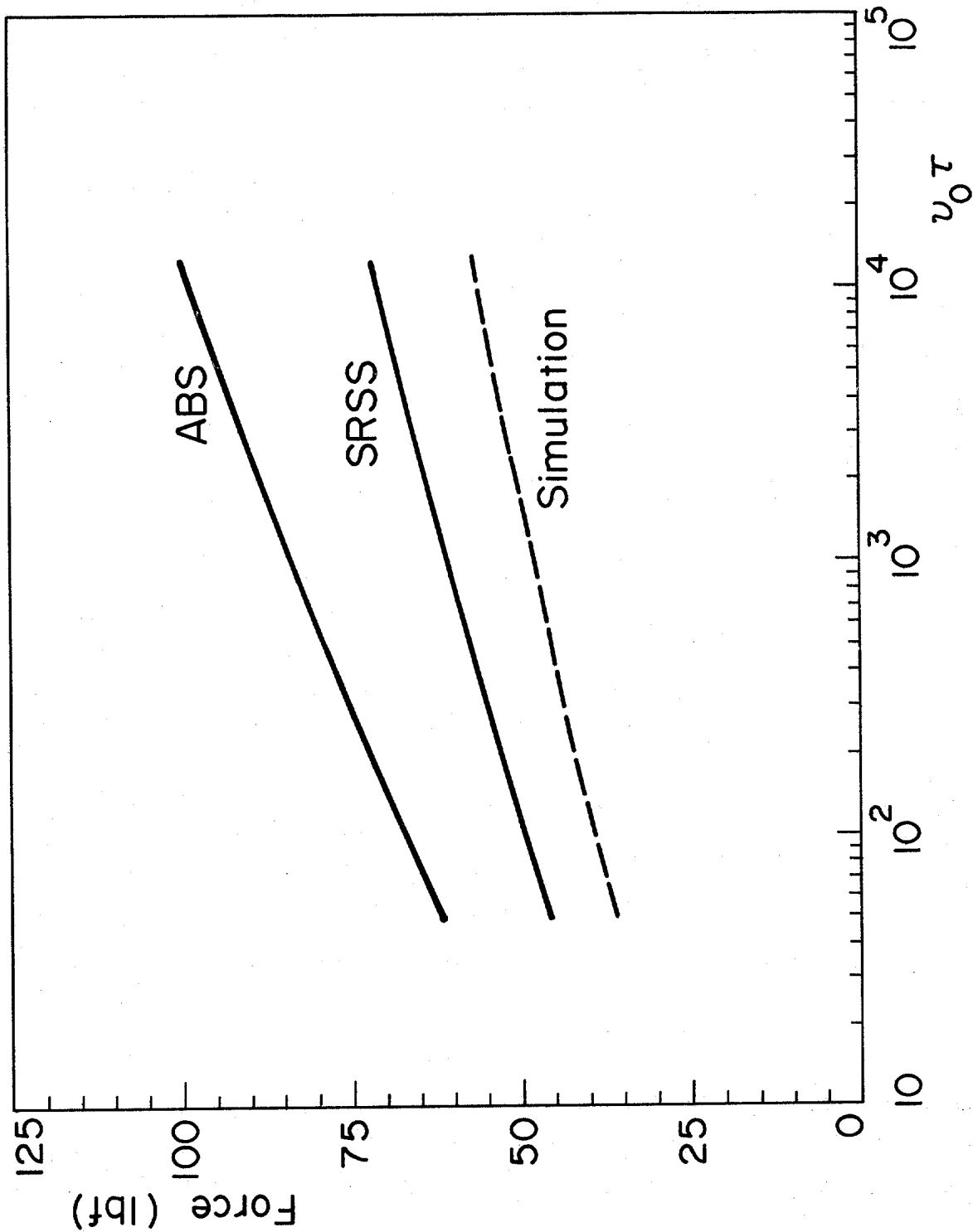


Figure 4(a). Exact and Approximate Means of Peak Wave Forces
(Band-Limited Wave Spectrum with $q = 0.5$, $\beta = 10$,
and $\alpha = 1$)

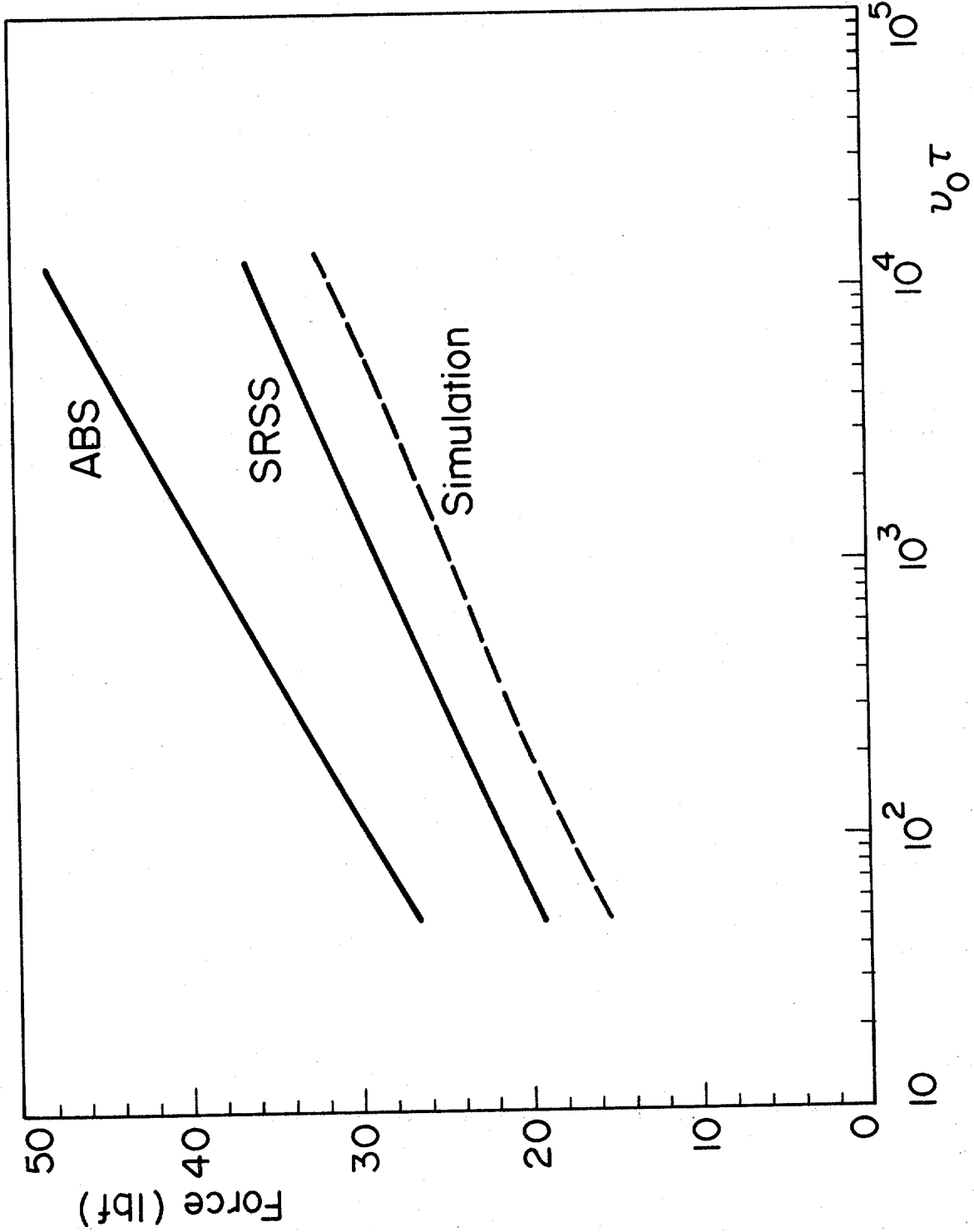


Figure 4(b). Exact and Approximate Means of Peak Wave Forces (Band-Limited Wave Spectrum with $q = 0.5$, $\beta = 10$, and $\alpha = 2$)

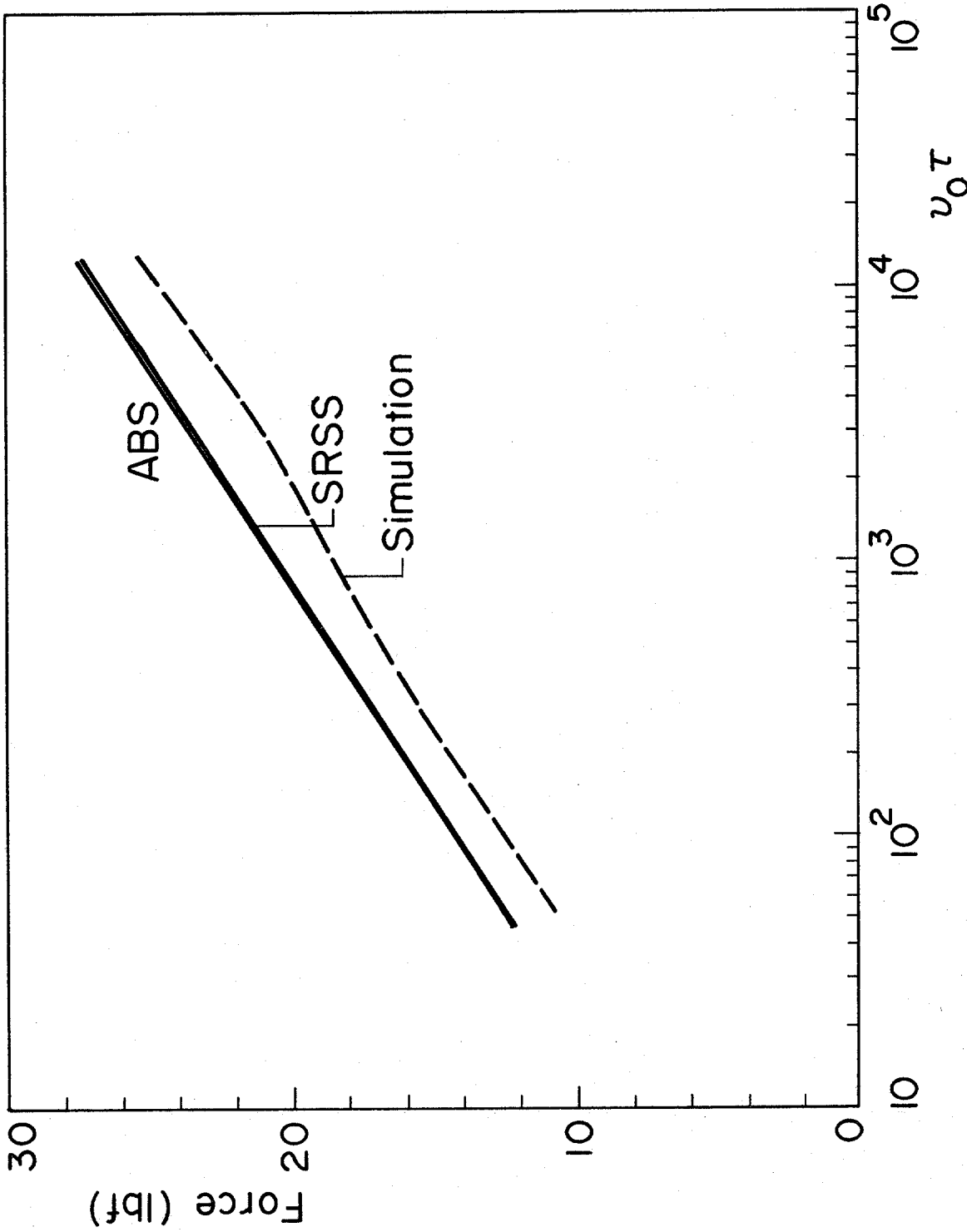


Figure 4(c). Exact and Approximate Means of Peak Wave Forces (Band-Limited Wave Spectrum with $q = .5$, $\beta = 10$, and $\alpha = 20$)

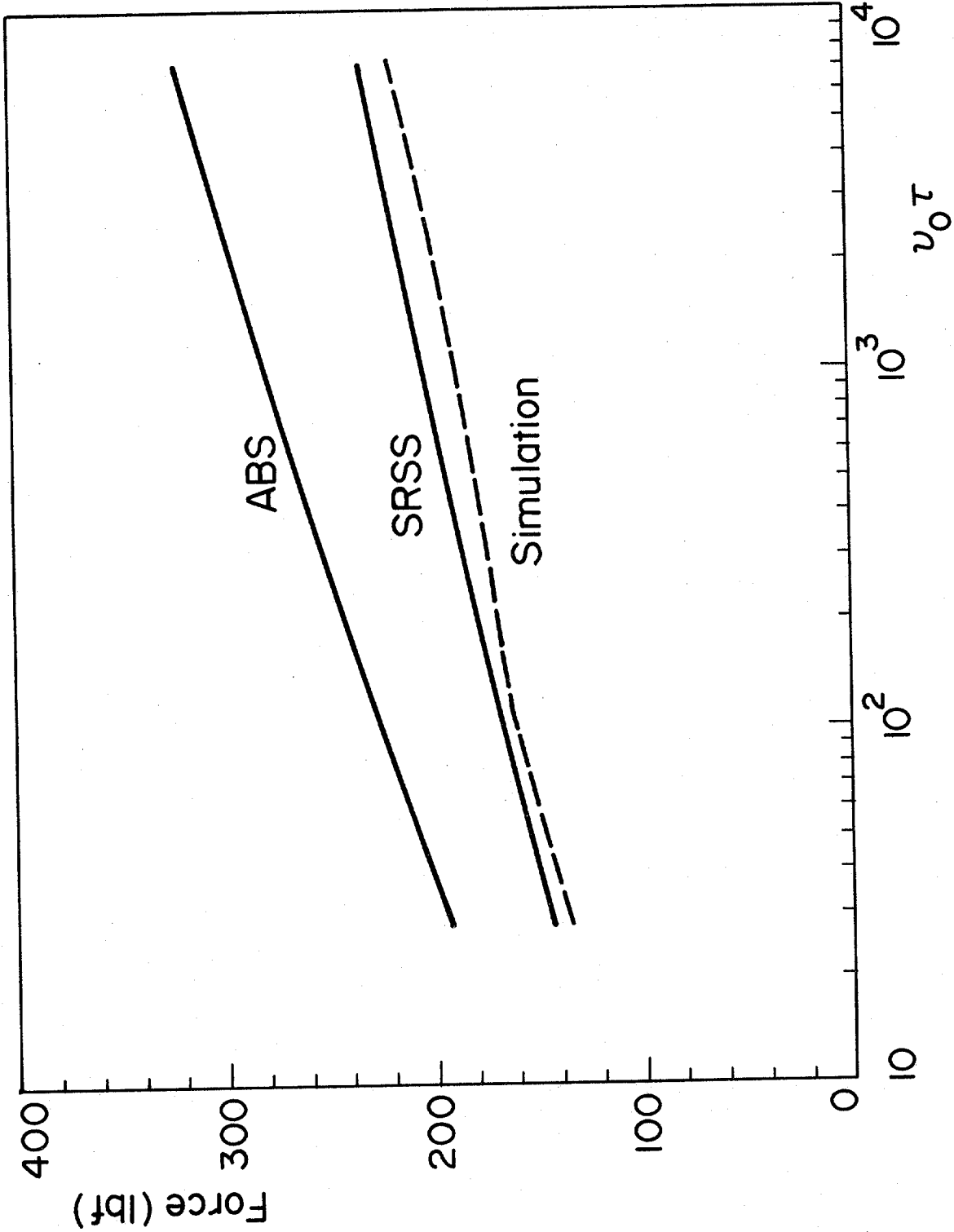


Figure 5(a). Exact and Approximate Means of Peak Wave Forces
(Pierson-Moskowitz Wave Spectrum with $v = 20$ knots,
 $q = 0.39$, $\beta = 10$, and $\alpha = 1$)

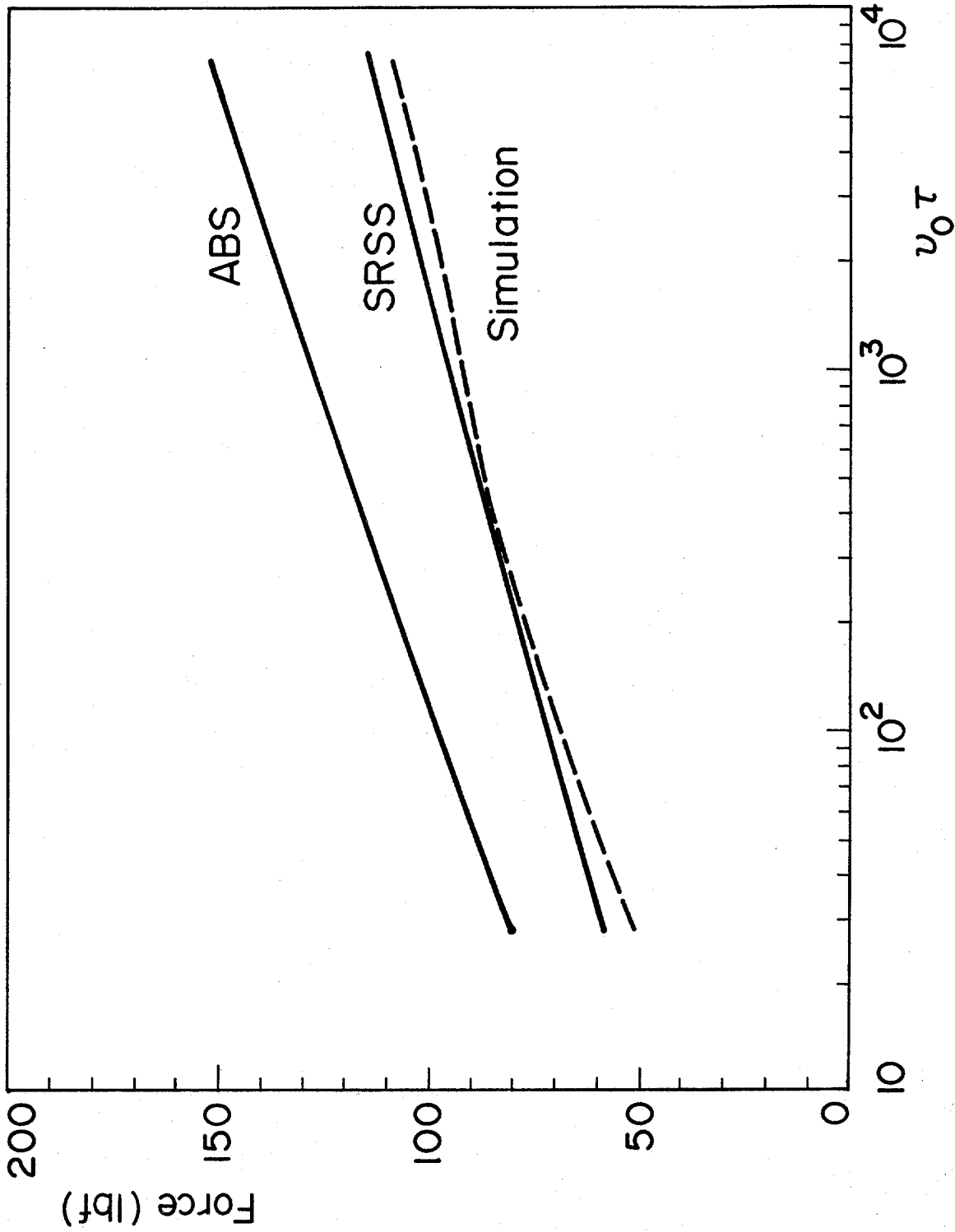


Figure 5(b). Exact and Approximate Means of Peak Wave Forces
(Pierson-Moskowitz Wave Spectrum with $v = 20$ knots,
 $q = 0.39$, $\beta = 10$, and $\alpha = 2$)

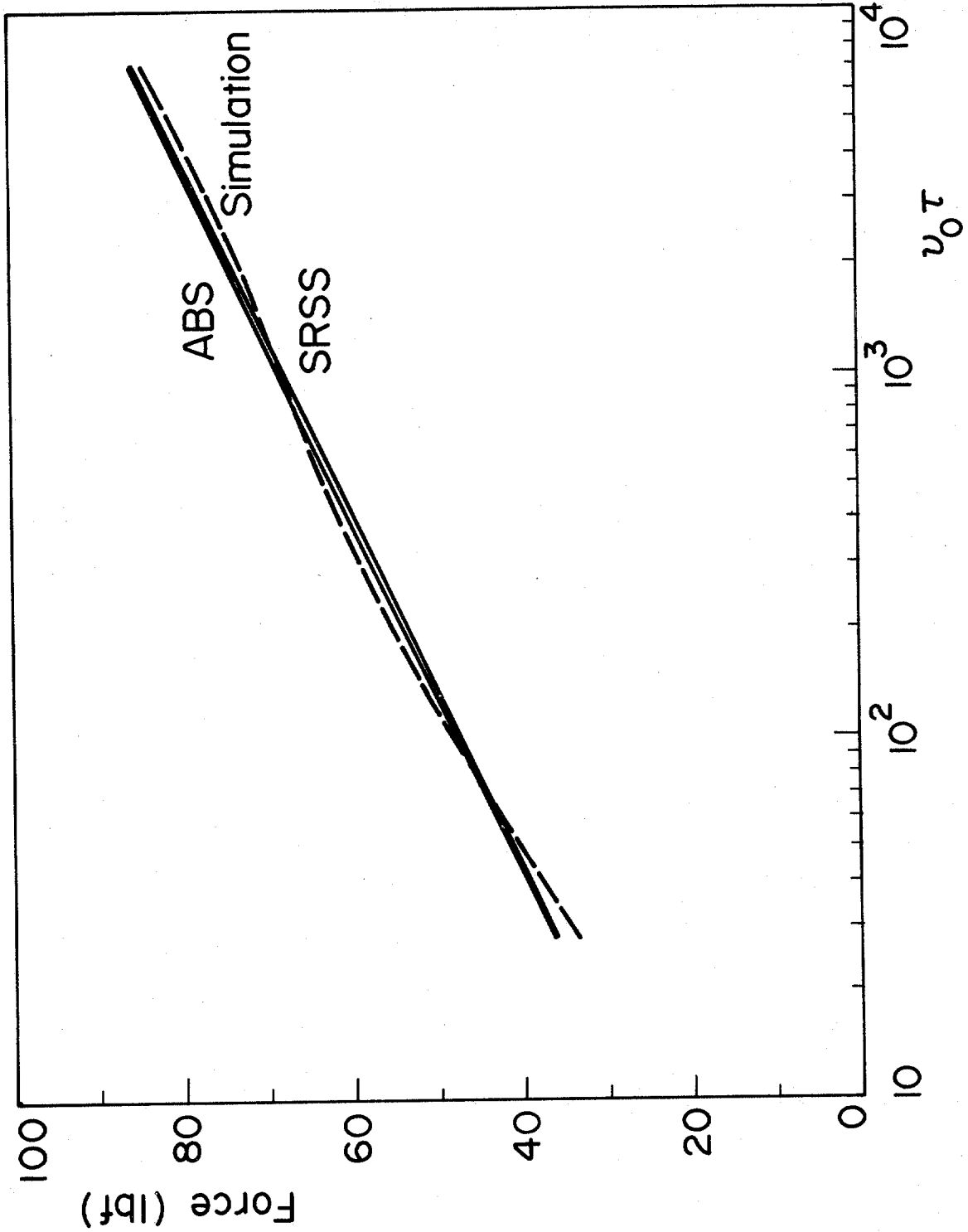


Figure 5(c). Exact and Approximate Means of Peak Wave Forces
(Pierson-Moskowitz Wave Spectrum with $v = 20$ knots,
 $q = 0.39$, $\beta = 10$, and $\alpha = 20$)

APPENDIX A
EXTREMES OF WAVE FORCES

EXTREMES OF WAVE FORCES

By Mircea Grigoriu

INTRODUCTION

According to Morison's equation, wave forces acting on cylindrical members have two components: drag forces, which depend nonlinearly on wave particle velocity, and inertia forces, which are proportional to wave particle acceleration (1, 7, 8, 9, 11, 12). Wave forces are then non-Gaussian processes although fluid velocities are assumed to follow Gaussian distributions. Yet, they are modeled by Gaussian processes when the analysis is based on statistical linearization because in this approach drag forces are approximated by linear functions of wave particle velocities (1, 7, 8, 9, 11).

The Gaussian hypothesis was examined extensively in the past and probabilistic characteristics were developed for individual peaks of wave forces and the largest value of these forces during storms (1, 7, 9, 10, 12, 13, 14). The analysis of extreme wave forces was often based on the assumption that individual peaks are independent (1, 12, 13, 14). Mean crossing rates of the wave force process (9, 10) and simulation (7) were also applied to determine maxima of wave forces. Developments generally consider the case of small or inexistent currents and assume that Morison's equation is valid.

This paper develops probabilistic descriptors for wave force processes characterized by Morison's equation, e.g., marginal distributions, mean crossing rates, and extreme value distributions, and evaluates further the Gaussian hypothesis. The descriptors are general and simple. They have closed-forms for drag forces with or without current and involve a single numerical integration when drag and inertia forces are considered simultaneously. Results can

be applied directly to the analysis of the quasi-static response of offshore platforms when Morison's equation is valid.

WAVE FORCES

Let $Y^*(t)$ be the wave particle velocity at any time t . It is assumed that $Y^*(t)$ is a twice-differentiable, stationary Gaussian process with positive mean y_0 , variance σ_Y^2 , and autocovariance function $B_Y(\tau) = \sigma_Y^2 \rho_Y(\tau)$. The process will be viewed in the analysis as the sum of two components, the current, y_0 , and the zero-mean fluctuating component, $Y(t)$,

$$Y^*(t) = y_0 + Y(t) \quad (1)$$

The variances of $\dot{Y}(t) = dY(t)/dt$ and $\ddot{Y}(t) = d^2Y(t)/dt^2$, which are needed to characterize inertia forces, can be determined from the following expressions (8)

$$\sigma_{\dot{Y}}^2 = -\sigma_Y^2 \left. \frac{d^2}{d\tau^2} \rho(\tau) \right|_{\tau=0} \quad (2)$$

$$\sigma_{\ddot{Y}}^2 = \sigma_Y^2 \left. \frac{d^4}{d\tau^4} \rho_Y(\tau) \right|_{\tau=0}$$

According to Morison's equation (1, 7, 12, 13), wave forces are proportional to

$$R(t) = X_1(t) + X_2(t) \quad (3)$$

in which the process

$$X_1(t) = (y_0 + Y(t)) \left| y_0 + Y(t) \right| \quad (4)$$

denotes drag forces and

$$X_2(t) = a \dot{Y}(t) \quad (5)$$

characterizes inertia forces. The coefficient a is a measure of the relative importance of inertia forces with respect to drag forces, e.g., inertia forces are negligible for small values of a .

DRAG FORCES

From Eq. 4, the drag force is a stationary non-Gaussian process whose characteristics can be determined from the probability law of the fluctuating component of flow velocity and the current.

Marginal Probabilistic Characteristics

The instantaneous density, f_1 , of $X_1(t)$ is independent of time since the drag force process is stationary. It can be obtained from Eq. 4 and characteristics of $Y(t)$ by elementary transformations which are discussed in most texts of probability theory (8). According to these transformations

$$f_1(x) = \frac{1}{\sqrt{2\pi} \sigma_Y |g'(g^{-1}(x))|} \exp \left[-\frac{1}{2} \left(\frac{g^{-1}(x) - y_0}{\sigma_Y} \right)^2 \right] \quad (6)$$

in which $x = g(y) = (y_0 + y) |y_0 + y|$. The marginal density of $X_1(t)$ can also be given in the form

$$f_1(x) = \frac{1}{2\sigma_Y \sqrt{2\pi|x|}} \exp \left\{ -\frac{1}{2} \left[\frac{\text{sgn}(x)\sqrt{|x|} - y_0}{\sigma_Y} \right]^2 \right\} \quad (7)$$

in which $\text{sgn}(x) = -1; 0; \text{ or } 1$ when x takes on negative, zero, or positive

values. This density is symmetric about $x = 0$ only when $y_0 = 0$. The mean, m_1 , and the variance, σ_1^2 , of the response can be determined from the first and second moments of the density in Eq. 7, i.e., the integrals

$$m_1 = \frac{y_0^2}{\sqrt{2\pi}} \left[\int_{-1/\alpha}^{\infty} (1+\alpha z)^2 \exp(-z^2/2) dz - \int_{1/\alpha}^{\infty} (1-\alpha z)^2 \exp(-z^2/2) dz \right] \quad (8)$$

$$\sigma_1^2 + m_1^2 = \frac{y_0^4}{\sqrt{2\pi}} \left[\int_{-1/\alpha}^{\infty} (1+\alpha z)^4 \exp(-z^2/2) dz + \int_{1/\alpha}^{\infty} (1-\alpha z)^4 \exp(-z^2/2) dz \right] \quad (9)$$

in which

$$\alpha = \sigma_Y/y_0 \quad (10)$$

Note that α is nearly zero when the current is dominant but approaches infinity as $y_0 \rightarrow 0$ for finite values of σ_Y . In the latter case, $m_1 = 0$ and $\sigma_1^2 + m_1^2 = \sigma_1^2 = 3\alpha^4$ because $y_0^2 (1 \pm \alpha z)^2 \rightarrow \alpha_Y^2 z^2$, $y_0^4 (1 \pm \alpha z)^4 \rightarrow \alpha_Y^4 z^4$, and $1/\alpha \rightarrow 0$ when the current vanishes.

The mean and variance of the response can be calculated simply from Eqs. 8 and 9 the following closed-form integrals

$$\int_{\alpha}^{\infty} (1 \pm \alpha z)^2 \exp(-z^2/2) dz = \sqrt{2\pi} (1 + \alpha^2) \phi^c(a/\sqrt{2}) + (a\alpha^2 + 2\alpha) \exp(-a^2/2) \quad (11)$$

$$\int_{\alpha}^{\infty} (1 \pm \alpha z)^4 \exp(-z^2/2) dz = \sqrt{2\pi} (1 + 6\alpha^2 + 3\alpha^4) \phi^c(a/\sqrt{2}) + [a\alpha^4(a^3 + 3) + 4\alpha^3(a^2 + 2) + 6a\alpha^2 + 4\alpha] \exp(-a^2/2) \quad (12)$$

where Φ^C = the complementary cumulative distribution function of the standard Gaussian variable. Table 1 gives values of the mean and standard deviation of the drag force scaled by y_0^2 , i.e., the dimensionless coefficients

$$\begin{aligned}\xi &= m_1/y_0^2 \\ \zeta &= \sigma_1/y_0^2\end{aligned}\tag{13}$$

for selected values of α . They are obtained from Eqs. 8 to 12 and are defined when the current is not zero.

The mean and the variance of $X_1(t)$ can be obtained approximately from linearized expressions of the drag force. For positive values of y_0 , one such expression is $y_0^2 + 2y_0 Y(t)$. It approximates the mean and the variance of the drag force by y_0^2 and $4\sigma_y^2 y_0^2 = 4\alpha^2 y_0^2$. The corresponding dimensionless coefficients in Eq. 13 can then be approximated by $\xi \approx 1.0$ and $\zeta = 2\alpha$. From Table 1, the approach provides satisfactory second-moment descriptors for $X_1(t)$ when $\alpha \leq 0.5$.

Mean Crossing Rates

The mean upcrossing rate of level x of $X_1(t)$, $v_1(x)$, can be obtained simply from developments in Ref. 5 related to nonlinear transformation of Gaussian processes. From this reference and the observation that there is a one-to-one correspondence between drag forces and flow velocities, one finds

$$v_1(x) = \frac{1}{2\pi} \frac{\sigma_y}{\alpha y_0} \exp \left\{ -\frac{1}{2} \left[\frac{\text{sgn}(x) \sqrt{|x|} - y_0}{\alpha y_0} \right]^2 \right\}\tag{14}$$

or

$$v_1(\tilde{x}) = v_0 \exp \left\{ -\frac{1}{2} \left[\frac{\operatorname{sgn}(\xi + \zeta \tilde{x}) \sqrt{|\xi + \zeta \tilde{x}| - 1}}{\alpha} \right]^2 \right\} \quad (15)$$

$$v_0 = \frac{1}{2\pi} \frac{\sigma_{\dot{Y}}}{\sigma_Y} = \frac{\sqrt{-\rho_Y''(0)}}{2\pi} \quad (16)$$

The standardized threshold, \tilde{x} , gives the number of standard deviation, σ_1 , from m_1 to x and can be determined from

$$x = m_1 + \sigma_1 \tilde{x} = y_0^2 (\xi + \zeta \tilde{x}) \quad (17)$$

Let $v_1^G(x)$ be the mean upcrossing rate of level x of the drag force under the Gaussian hypothesis. According to this hypothesis, $X_1(t)$ is a Gaussian process. The corresponding mean upcrossing rate function has the expression (8, 11)

$$v_1^G(\tilde{x}) = \frac{1}{2\pi} \frac{\dot{\sigma}_1}{\sigma_1} \exp \left(-\frac{1}{2} \tilde{x}^2 \right) \quad (18)$$

in which $\dot{\sigma}_1$ = the standard deviation of $\dot{X}_1(t) = dX_1(t)/dt$. From Eq. 4, the time-derivative of the drag force process is

$$\dot{X}_1(t) = 2|y_0 + Y(t)| \dot{Y}(t) \quad (19)$$

for all values of y_0 and $Y(t)$. Since $Y(t)$ and $\dot{Y}(t)$ are independent, the process $\dot{X}_1(t)$ has the mean zero and variance

$$\sigma_1^2 = 4 \sigma_Y^2 y_0^2 (1 + \alpha^2) \quad (20)$$

The mean upcrossing rate in Eq. 18 can also be given in the form (Eqs. 13 and 20)

$$v_1^G(\bar{x}) = v_0 \frac{2\alpha\sqrt{1+\alpha^2}}{\zeta} \exp\left(-\frac{1}{2} \bar{x}^2\right) \quad (21)$$

The ratio between the exact and the approximate mean upcrossing rates, v_1 and v_1^G in Eqs. 15 and 21, has the expression

$$\frac{v_1(\bar{x})}{v_1^G(\bar{x})} = \frac{\zeta}{2\alpha\sqrt{1+\alpha^2}} \exp\left\{-\frac{1}{2} \left[\left(\frac{\sqrt{\xi + \zeta \bar{x}} - 1}{\alpha} \right)^2 + \bar{x} \right] \right\} \quad (22)$$

for positive values of \bar{x} . Figure 1 shows the variation of the ratio v_1/v_1^G in Eq. 22 with the standardized threshold, \bar{x} , for several values of α . Note that the Gaussian hypothesis results in unconservative approximations of the mean upcrossing rate. The degree of unconservatism increases with the threshold and the value of α (larger values of α correspond to smaller currents). For example, v_1/v_1^G is approximately 6.4 and 100 at $\bar{x} = 4.0$ when $\alpha = 0.1$ and 0.5, respectively. Note also that the ratio v_1/v_1^G is nearly independent of α and approximately equal to its value for $\alpha = \infty$ (zero current) when α exceeds 0.5. Values of α in excess of 0.5 are common in design.

Largest Value Distribution

It is generally convenient to develop for design purposes other descriptors of the peak wave forces, in addition to the mean upcrossing rate. Let $X_{1,\tau}$ be the maximum drag force during a storm of duration τ and denote by

$$\tilde{X}_{1,\tau} = \frac{X_{1,\tau} - m_1}{\sigma_1} \quad (23)$$

The cumulative distribution function of $X_{1,\tau}$ at x can be determined from the probability that the drag force is smaller than x at $t = 0$, i.e., $X_1(0) \leq x$, and the number of upcrossings of threshold x of $X_1(t)$ during $[0, \tau]$, $N_\tau(x)$, is zero. This probability can be determined simply if it is assumed that the variables $X_1(0)$ and $N_\tau(x)$ are independent and the upcrossings of level x of $X_1(t)$ follow a Poisson process. The assumptions are satisfactory for relatively high thresholds (8, 15) and provide the following expression for the distribution $F_{1,\tau}$ of $\tilde{X}_{1,\tau}$

$$F_{1,\tau}(\tilde{x}) = F_1(\tilde{x}) \exp [- (v_0 \tau) \delta(\tilde{x})] \quad (24)$$

This function depends on $\delta(\tilde{x}) = v_1(\tilde{x})/v_0$ with $v_1(\tilde{x})$ in Eq. 15 and the marginal distribution of $\tilde{X}_1(t) = (X_1(t) - m_1)/\sigma_1$ which has the form

$$F_1(\tilde{x}) = \Phi \left(\frac{\text{sgn}(\xi + \zeta \tilde{x}) \sqrt{|\xi + \zeta \tilde{x}|} - 1}{\alpha} \right) \quad (25)$$

in which Φ = the cumulative distribution function of the standard Gaussian variable. The density of $\tilde{X}_{1,\tau}$, $f_{1,\tau}$, can be obtained by differentiating Eq.24

$$f_{1,\tau}(\tilde{x}) = \delta(\tilde{x}) \exp [- (v_0 \tau) \delta(\tilde{x})] \left\{ \frac{\zeta}{2\alpha \sqrt{2\pi} |\xi + \zeta \tilde{x}|} + \right. \\ \left. + (v_0 \tau) \frac{\zeta \text{sgn}(\xi + \zeta \tilde{x}) \sqrt{|\xi + \zeta \tilde{x}|} - 1}{2\alpha^2 \sqrt{|\xi + \zeta \tilde{x}|}} F_1(\tilde{x}) \right\} \quad (26)$$

Similar considerations can be applied when Gaussian drag forces are postulated. In this case, the density $f_{1,\tau}^G$ of $\tilde{x}_{1,\tau}$ has the expression

$$f_{1,\tau}^G(\tilde{x}) = \left[\frac{1}{\sqrt{2\pi}} + (v_0\tau) \tilde{x} \Phi(\tilde{x}) \right] \exp \left\{ -\frac{\tilde{x}^2}{2} - (v_0\tau) e^{-\tilde{x}^2/2} \right\} \quad (27)$$

Figure 2 shows the densities $f_{1,\tau}$ and $f_{1,\tau}^G$ with solid and dotted lines for $v_0\tau = 200, 4000, \text{ and } 40000$. They are referred to as exact and Gaussian results. Note that the Gaussian hypothesis underestimates in the average the peak response even when the current is large ($\alpha = 0.5$).

The densities in Eqs. 26 and 27 were used to determine by numerical integration the mean, the standard deviation, the coefficient of skewness, and the coefficient of kurtosis of the peak drag force. Figure 3 shows the variation of these moments with $v_0\tau$ for $\alpha = 0.5$. Similar results were found for other values of α . The means and the standard deviations plotted in this figure are divided y_0^2 . Note that the Gaussian hypothesis yields approximations which underestimates significantly the mean and the standard deviation of the peak wave force. For example, the exact values of the mean, the standard deviation, the coefficient of skewness, and the coefficient of kurtosis are $10.4 y_0^2, 0.86 y_0^2, 1.06, \text{ and } 5.05$ for $\alpha = 0.5$ and $v_0\tau = 10,000$. These moments are approximated by $6.0 y_0^2, 0.26 y_0^2, 0.88, \text{ and } 4.38$ when the Gaussian hypothesis is applied. The use of this hypothesis in analysis is likely to result in unconservative designs.

Asymptotic approximations (as $v_0\tau \rightarrow \infty$) can be developed for the mean and variance of the peak drag force process when this process is assumed to be Gaussian. They are (2)

$$m_{1,\tau}^G = y_0^2 \left[\xi + \zeta \left(\sqrt{2 \ln(v_0 \tau)} + \frac{0.577216}{\sqrt{2 \ln(v_0 \tau)}} \right) \right] \quad (28)$$

$$\sigma_{1,\tau}^G = y_0^2 \sqrt{\frac{\pi}{6} \frac{\zeta}{2 \ln(v_0 \tau)}} \quad (29)$$

The approximate means and variances in these equations coincide practically with corresponding parameters in Fig. 3, which were obtained by numerical integration.

DRAG AND INERTIA FORCES

The general wave force in Eqs. 3 to 5 is examined in this section. Note that the drag and the inertia forces, $X_1(t)$ and $X_2(t)$, are independent at any time t because $Y(t)$ and $\dot{Y}(t)$ are uncorrelated Gaussian processes. From Eqs. 3, 13, and 20, the mean and the variance of $R(t)$ are

$$m_R = \xi y_0^2 \quad (30)$$

$$\sigma_R^2 = (\zeta^2 + \beta^2) y_0^4 \quad (31)$$

while the variance of the time-derivative of the wave force has the expression

$$\sigma_{\dot{R}}^2 = [4(1+\alpha^2) + \sigma^2] \sigma_Y^2 y_0^2 \quad (32)$$

These equations are valid when the current is not zero. When there is no current, $m_R = 0$, $\sigma_R^2 = 3\sigma_Y^4 + \alpha_Y^2$, and $\sigma_{\dot{R}}^2 = 4\sigma_Y^2 \sigma_Y^2 + a^2 \sigma_Y^2$. The parameter β in Eq. 31 quantifies the importance of inertia forces with respect to drag forces associated with the current and is equal to

$$\beta = \frac{a\sigma_Y^*}{y_0^2} = \frac{a\alpha}{y_0} \frac{\sigma_Y^*}{\sigma_Y} \quad (33)$$

δ is a derived parameter which has the following expression

$$\delta = \frac{\sigma_Y a}{\sigma_Y^* y_0} = \frac{\beta}{\alpha} \frac{\sigma_Y^* \sigma_Y}{\sigma_Y^2} \quad (34)$$

From Eqs. 33 and 34, β and δ depend on the correlation structure or, equivalently, the power spectral density of $Y(t)$. This dependence is examined in Table 2 for monochromatic, narrow-band, and wide-band wave particle velocities, $Y(t)$, for the case in which $\sigma_Y^2 = 1.0$. Results show that the ratio σ_Y/σ_Y^2 depends weakly on the shape of the power spectral density of $Y(t)$. Thus, δ is primarily a function of the relative importance of inertia and drag forces, i.e., the ratio a/y_0 . The parameters α , β , and δ can be determined simply from the ratio, a , between the inertia and drag coefficients, the current y_0 , and the spectral characteristics of flow velocity.

Mean Crossing Rates

The mean upcrossing rate of level r of $R(t)$, $v(r)$, can be determined exactly from the mean rate at which the vector process $\{X_1(t), X_2(t)\}$ leaves the two-dimensional domain $\{(x_1, x_2) : x_1 + x_2 \leq r\}$ (3, 16). For simplicity, v is approximated in this section from the point-crossing formula. According to this formula, v can be approximated by (6, 17)

$$v^*(r) = \int_{-\infty}^{\infty} f_2(x_2) v_1(r-x_2) dx_2 + \int_{-\infty}^{\infty} f_1(x_1) v_2(r-x_1) dx_1 \quad (35)$$

in which f_i and v_i denote the marginal density and the mean upcrossing rate functions of $X_i(t)$. The point-crossing formula has been applied successfully to the analysis of the combined effect of structural loads.

The marginal density and the mean upcrossing rate functions of $X_1(t)$, the drag force, are given in Eqs. 7 and 14. The corresponding functions of $X_2(t)$, the inertia force, can be determined simply because this process is Gaussian.

$$f_2(n) = \frac{1}{\sqrt{2\pi} a \sigma_{\dot{Y}}} \exp \left\{ -\frac{1}{2} \left[\frac{n}{a\sigma_{\dot{Y}}} \right]^2 \right\} \quad (36)$$

and

$$v_2(n) = \frac{1}{2\pi} \frac{\sigma_{\dot{Y}}}{\sigma_Y} \exp \left\{ -\frac{1}{2} \left[\frac{n}{\alpha\sigma_{\dot{Y}}} \right]^2 \right\} \quad (37)$$

From Eq. 35, the mean upcrossing rate $v(r)$ can be approximated by

$$v^*(\tilde{r}) = v_0 \frac{1}{\sqrt{2\pi} \beta} v^{**}(\tilde{r}) \quad (38)$$

in which $\tilde{r} = (r - m_R)/\sigma_R$ with m_R and σ_R in Eqs. 30 and 31,

$$v^{**}(\tilde{r}) = \int_{-\infty}^{\infty} \left\{ \exp \left[-\frac{1}{2} \left(\left(\frac{u}{\beta} \right)^2 + \frac{(\text{sgn}(\tilde{r}-u) \sqrt{|\tilde{r}-u|} - 1)^2}{\alpha} \right) \right] + \right. \\ \left. + \delta \exp \left[-\frac{1}{2} \left(\left(\frac{u-1}{\alpha} \right)^2 + \frac{(\tilde{r}-\text{sgn}(u)u)^2}{\beta} \right) \right] \right\} du \quad (39)$$

and $\tilde{r} = r/y_0^2 = \xi + \tilde{r} \sqrt{\zeta^2 + \beta^2}$.

The mean upcrossing rate of the wave force, when assumed to be a Gaussian process, can still be determined from Eq. 18, in which σ_R and σ_R^* are given by Eqs. 31 and 32. It has the expression

$$v_G(\tilde{r}) = v_0 \alpha \sqrt{\frac{4(1+\alpha^2)+\delta^2}{\xi_2^2+\beta^2}} \exp\left(-\frac{1}{2} \tilde{r}^2\right) \quad (40)$$

and involves only second-moment characteristics of the response and its time-derivative.

From Eqs. 38 to 40, the ratio between the mean upcrossing rates v^* and v_G is

$$\frac{v^*(\tilde{r})}{v_G(\tilde{r})} = \frac{1}{\sqrt{2\pi} \alpha \beta} \sqrt{\frac{\xi_2^2+\beta^2}{4(1+\alpha^2)+\delta^2}} v^{**}(\tilde{r}) \exp\left(\frac{1}{2} \tilde{r}^2\right) \quad (41)$$

This result is applied to evaluate the Gaussian hypothesis although it involves approximations. However, the experience with the point-crossing formula (6, 17) shows that errors associated with this formula are much smaller than those due to the Gaussian assumption (Fig. 1). Thus, it is considered that Eq. 41 provides a satisfactory base for the evaluation of the Gaussian hypothesis when both drag and inertia forces act simultaneously.

Figure 4 shows the variation of v^*/v_G in Eq. 41 with \tilde{r} for $\sigma_u^2/\sigma_v^2 = 1.0$ (i.e., monochromatic excitation), $\alpha = 0.5$ and selected values of β . The ratio v^*/v_G increases with the threshold but decreases with β . For small values of β drag forces are dominant and, as expected, v^*/v_G and v_1/v_1^G in Fig. 1 are nearly equal. When inertia forces are significant β is large and the response

follows approximately a Gaussian distribution. In this case, the Gaussian hypothesis is satisfactory ($v/v_G^* = 1.0$). Similar results have been found for other types of excitations, e.g., the narrow- and wide-band processes in Table 2.

The mean crossing rate functions developed in this section can be applied as in Eqs. 26 and 27 to determine probabilistic characteristics of the peak wave force during storms. However, such developments are not presented in this paper.

CONCLUSIONS

Exact and approximate descriptors were determined for the Morison-type wave forces and their peaks during design storms. The approximations were based on the hypothesis that wave forces follow Gaussian distributions. It was assumed that the wave particle velocity can be modeled by a Gaussian process.

Results show that the Gaussian hypothesis, which is characteristic to the statistical linearization method, yields unsatisfactory descriptors for the peak wave force. Both the mean and the variance of this variable are generally underestimated. The Gaussian hypothesis is acceptable only when inertia forces are dominant because, in this special case, the wave force is approximately a Gaussian process.

REFERENCES

1. Borgman, L. E., "Statistical Models for Ocean Waves and Wave Forces," Advances in Hydroscience, Vol. 8, 1972, pp. 139-181.
2. Davenport, A. G., "Note on the Distribution of the Largest Value of a Random Function with Application to Just Loading," Proceedings, Instituti of Civil Engineers, London, Vol. 28, 1964, pp. 187-196.
3. Grigoriu, M., "Mean Failure Rate for Structural Systems Subjected to Time Dependent Loads," presented at the June 21-25, 1982, Ninth National Congress of Applied Mechanics, held at Ithaca, N.Y.

4. Grigoriu, M., "Dynamic Response of Offshore Platforms to Environmental Loads," Proceedings of the 4th ASCE Specialty Conference on Probabilistic Mechanics and Structural Reliability, American Society of Civil Engineers, January, 1984, pp. 115-118.
5. Grigoriu, M., "Crossings of Non-Gaussian Translation Processes," Journal of Engineering Mechanics, ASCE, Vol. 110, No. EM4, April 1984, pp. 610-620.
6. Larrabee, R. D., and Cornell, C. A., "Combination of Various Load Processes," Journal of the Structural Division, ASCE, Vol. 107, No. ST1, Proc. Paper 15999, Jan., 1981, pp. 223-239.
7. Larrabee, R. D., "Extreme Wave Dynamics of Deepwater Platforms," presented at the August 1982, 3rd International Conference on Behavior of Offshore Structures, BOSS 82, held at Cambridge, Mass.
8. Lin, Y. K., Probabilistic Theory of Structural Mechanics, Robert E. Krieger Publishing Company, Huntington, NY, 1976.
9. Moe, G., and Crandall, S. H., "Extremes of Morison-Type Wave Loading on Simple Pile," Translations of the ASME, Vol. 100, Jan. 1978, pp. 100-104.
10. Moe, G., "Long-Term Wave Force Statistics for a Vertical Pile," Coastal Engineering, Vol. 2, 1979, pp. 297-311.
11. Rice, S. O., "Mathematical Analysis of Random Noise," Bell System Technical Journal, Vol. 24, 1945, pp. 46-156.
12. Tickell, R. G., "Continuous Random Wave Loading on Structural Members," The Structural Engineer, Vol. 55, No. 5, May, 1977, pp. 209-222.
13. Tickell, R. G., "The Probabilistic Approach to Wave Loading on Marine Structures," Mechanics of Wave-Induced Forces on Cylinders, T. L. Shaw, ed., Pitman Advanced Publishing Program, San Francisco, 1979, pp. 152-178.
14. Tung, C. C., "Peak Distribution of Random Wave-Current Force," Journal of the Engineering Mechanics Division, ASCE, Vol. 100, No. EM5, Proc. Paper 10843, Oct., 1976, pp. 873-884.
15. Vanmarcke, E. H., "Structural Response to Earthquakes," Seismic Risk and Engineering Decisions, C. Lmnitz and E. Rosenblueth, ed., Elsevier Publishing Co., Amsterdam, 1976, pp. 287-337.
16. Veneziano, D., Grigoriu, M., and Cornell, C. A., "Vector-Process Models for System Reliability," Journal of the Engineering Mechanics Division, ASCE, Vol. 103, No. EM3, Proc. Paper 12981, June, 1977, pp. 441-460.
17. Winterstein, S. R., "Combined Dynamic Responses: Extremes and Fatigue Damage," Research Report R80-46, Department of Civil Engineering, Massachusetts Institute of Technology, Cambridge, Mass., Dec., 1980.

Table 1. Mean and Variance Coefficients of Drag Forces

Coefficient	$\alpha = 0.1$	$\alpha = 0.3$	$\alpha = 0.5$	$\alpha = 1.0$	$\alpha = 2.0$
ξ	1.01	1.07082	1.10741	1.5250	2.7902
ζ	0.200499	0.625344	1.1018	2.5035	6.5858
2α	0.20	0.60	1.00	2.00	4.00

Table 2. Spectral Characteristics of Wave Particle Velocity

One-sided Spectral Density of $Y(t)$	$\frac{2}{\sigma_Y^2}$	$\frac{2}{\sigma_Y^2}$	σ_Y^*/σ_Y^2
$G_Y(\omega) = \begin{cases} 1.0 & , \omega = \omega_0 \\ 0.0 & , \text{otherwise} \end{cases}$	$\frac{2}{\omega_0^2}$	$\frac{4}{\omega_0^4}$	1.0
$G_Y(\omega) = \begin{cases} 1/\omega_c & , 0 \leq \omega \leq \omega_c \\ 0 & , \omega > \omega_c \end{cases}$	$\frac{\omega_c^2}{3}$	$\frac{\omega_c^4}{5}$	$\frac{3}{\sqrt{5}} = 1.3416$
$G_Y(\omega) = \begin{cases} 1/(\omega_b - \omega_a) & , \omega_a \leq \omega \leq \omega_b \\ 0.0 & , \text{otherwise} \end{cases}$ <p style="text-align: center;">$p = \omega_a/\omega_b$</p>	$\frac{\omega_b^2}{3}(p^2+p+1)$	$\frac{\omega_b^4}{5}(p^4+p^3+p^2+p+1)$	$\frac{3}{\sqrt{5}} \frac{\sqrt{p^4+p^3+p^2+p+1}}{p^2+p+1}$ <p>Note: $1.0 \leq \sigma_Y^*/\sigma_Y^2 \leq 3/\sqrt{5}$</p>

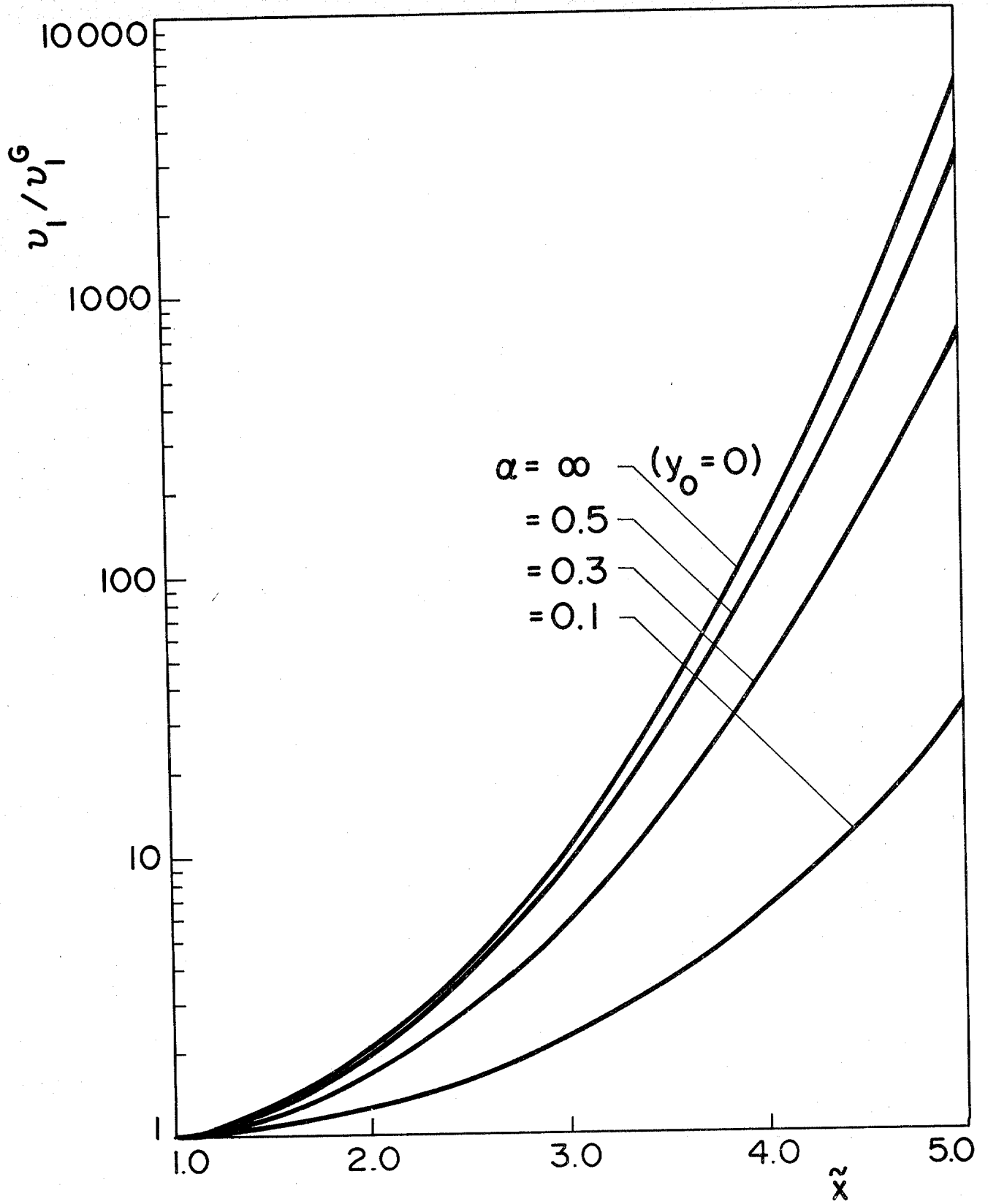


Figure 1. Ratio of Exact to Approximate Mean Upcrossing Rates of Drag Force

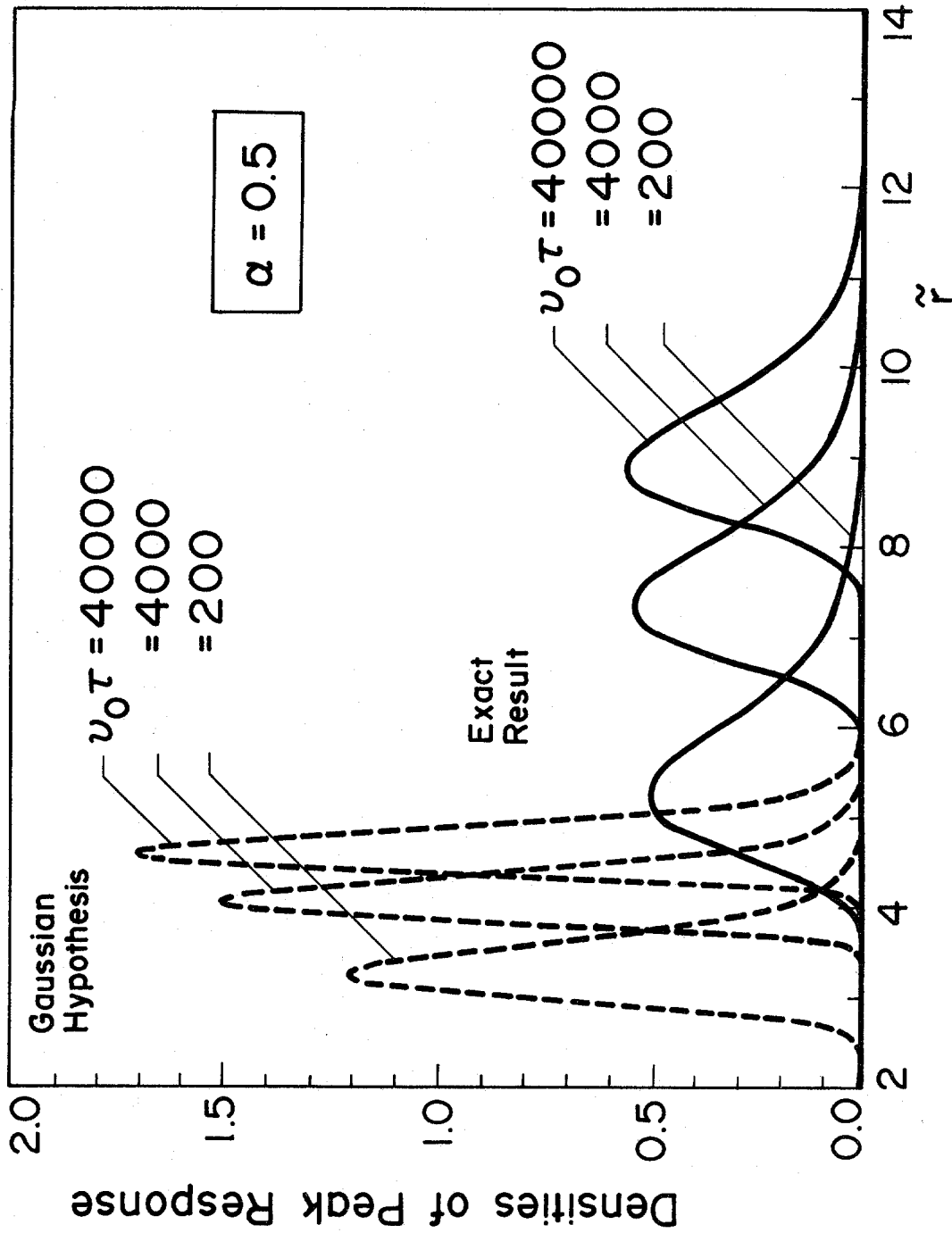


Figure 2. "Exact" and Approximate Probability Density Functions of Peak Drag Force

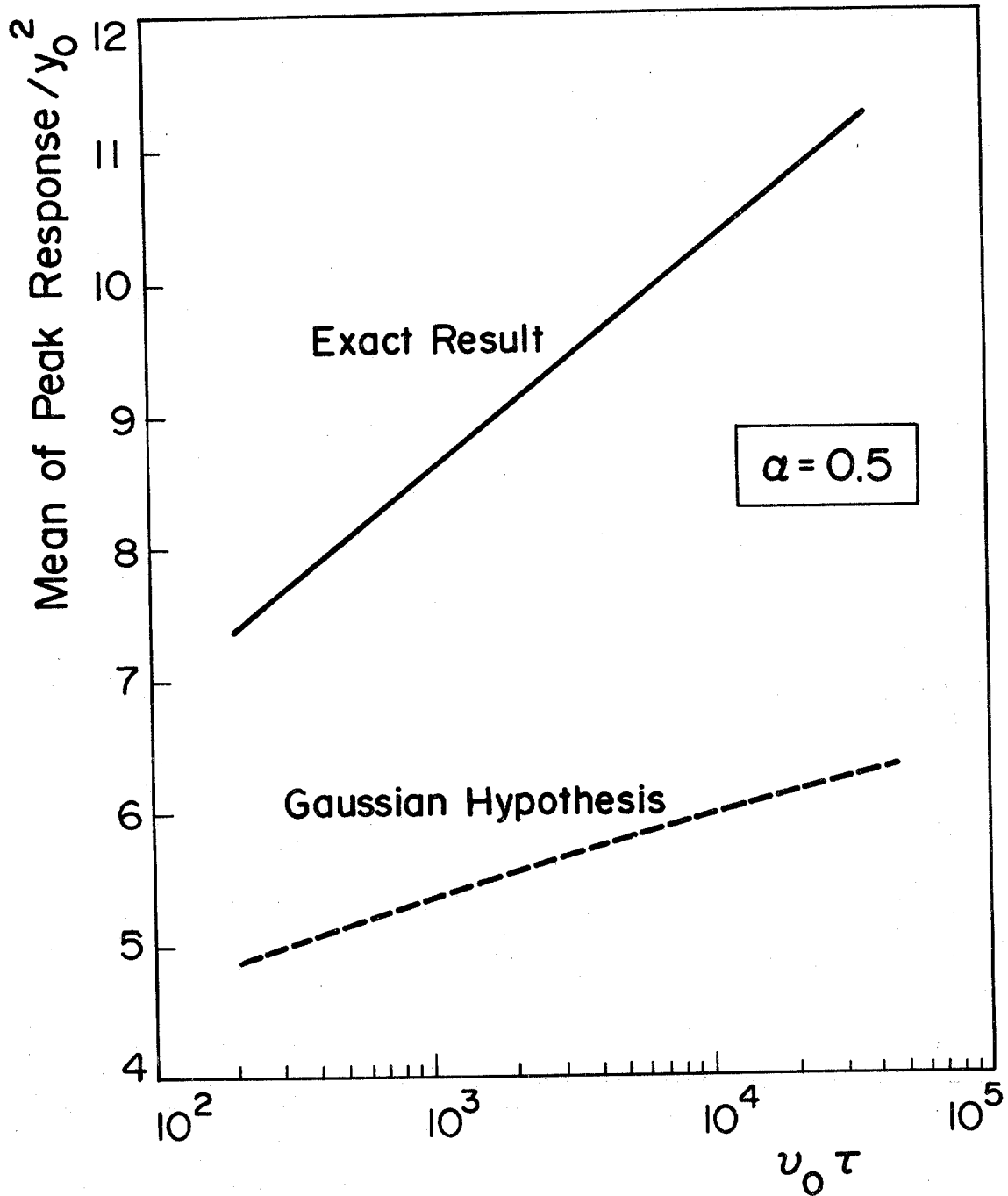


Figure 3(a). "Exact" and Approximate Moments of Peak Drag Force

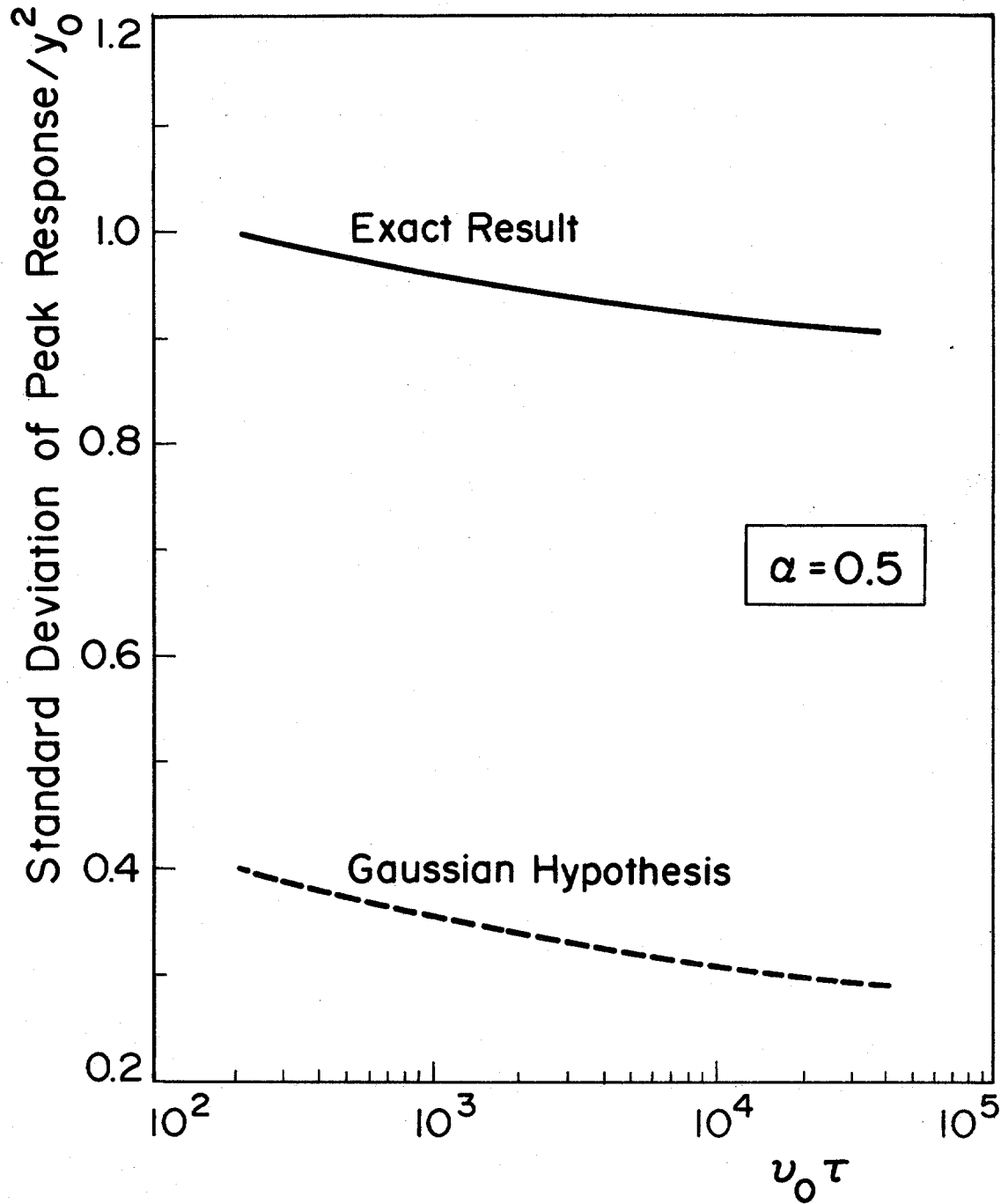


Figure 3(b). "Exact" and Approximate Moments of Peak Drag Force

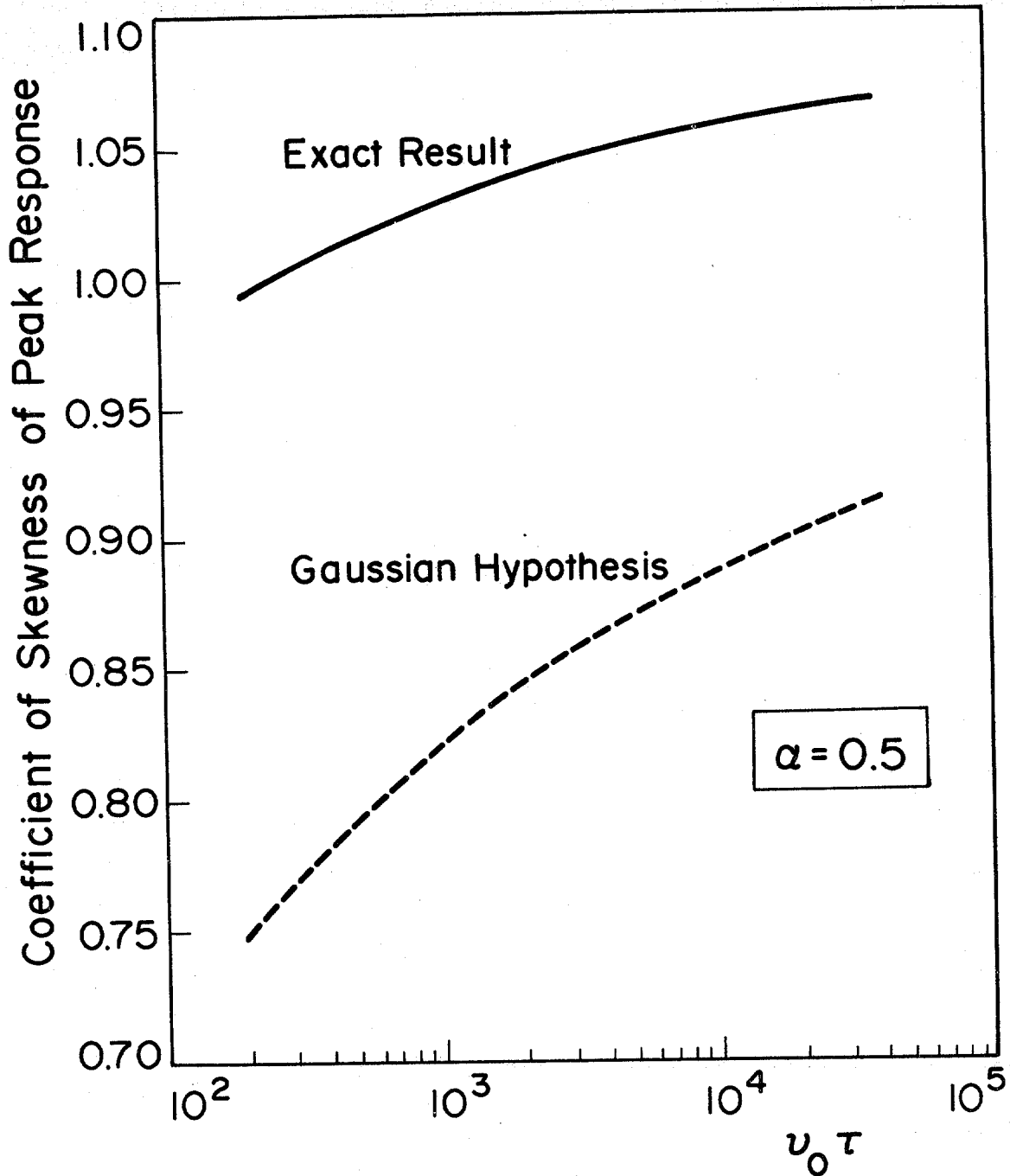


Figure 3(c). "Exact" and Approximate Moments of Peak Drag Force

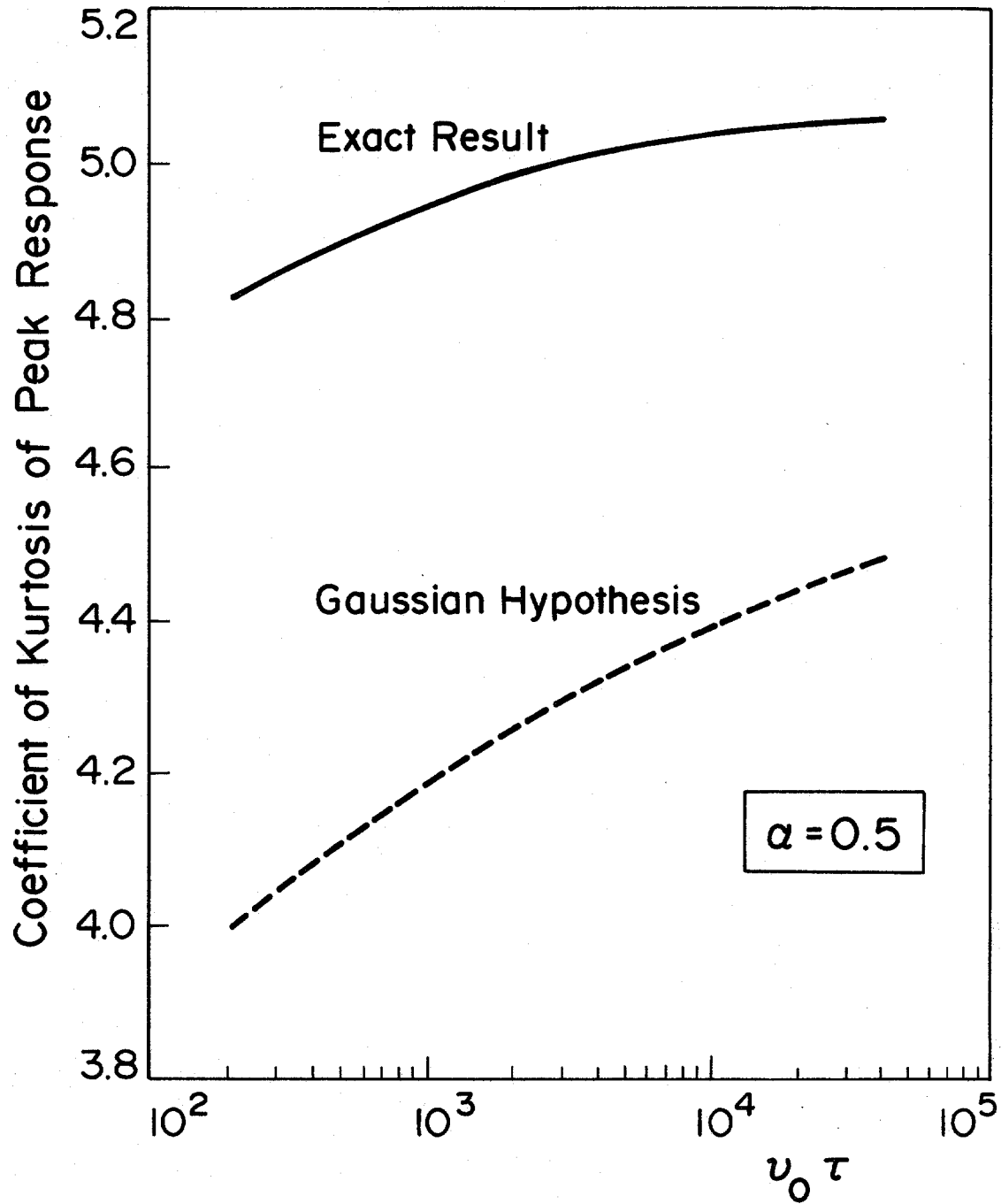


Figure 3(d). "Exact" and Approximate Moments of Peak Drag Force

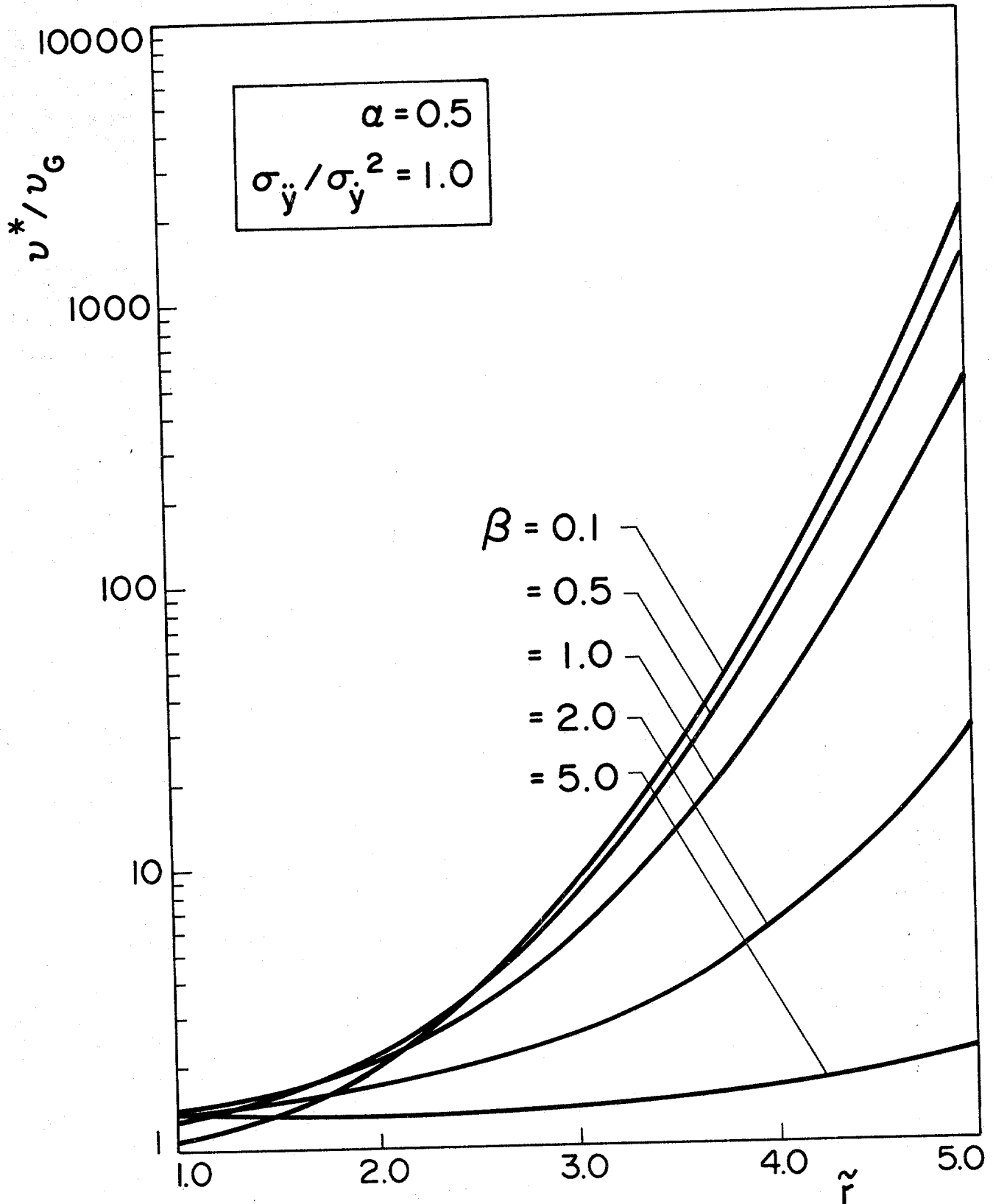


Figure 4. Ratio of "Exact" to Approximate Mean Upcrossing Rates of Drag and Inertia Forces

U.S. DEPT. OF COMM. BIBLIOGRAPHIC DATA SHEET <i>(See instructions)</i>	1. PUBLICATION OR REPORT NO. NBS/GCR-84/481	2. Performing Organ. Report No.	3. Publication Date
4. TITLE AND SUBTITLE Practical Approximations of Peak Wave Forces			
5. AUTHOR(S) Mircea Grigoriu and Bunu Alibe			
6. PERFORMING ORGANIZATION <i>(If joint or other than NBS, see instructions)</i> NATIONAL BUREAU OF STANDARDS DEPARTMENT OF COMMERCE WASHINGTON, D.C. 20234		7. Contract/Grant No.	8. Type of Report & Period Covered
9. SPONSORING ORGANIZATION NAME AND COMPLETE ADDRESS <i>(Street, City, State, ZIP)</i> Minerals Management Service Reston, VA 22091			
10. SUPPLEMENTARY NOTES <input type="checkbox"/> Document describes a computer program; SF-185, FIPS Software Summary, is attached.			
11. ABSTRACT <i>(A 200-word or less factual summary of most significant information. If document includes a significant bibliography or literature survey, mention it here)</i> According to Morison's equation, wave forces acting on cylindrical members have two components: drag forces, which depend nonlinearly on wave particle velocity, and inertia forces, which are proportional to wave particle acceleration. Wave forces are then non-Gaussian processes although fluid velocities are assumed to follow Gaussian distributions. This report develops approximations of the mean of the peak of wave forces during design storms. It shows that the square root of the sum of the squares (SRSS) rule can be applied to approximate the mean of the peak wave force from the average peaks of inertia and drag forces. The approximation is satisfactory for any ratio of drag to inertia forces and frequency content of the wave particle velocity process. The report also provides various descriptors of drag, inertia, and wave forces, including marginal distributions, mean crossing rates, and extreme value distributions.			
12. KEY WORDS <i>(Six to twelve entries; alphabetical order; capitalize only proper names; and separate key words by semicolons)</i> Extreme values; loads; ocean engineering; offshore structures; reliability; waves			
13. AVAILABILITY <input checked="" type="checkbox"/> Unlimited <input type="checkbox"/> For Official Distribution. Do Not Release to NTIS <input type="checkbox"/> Order From Superintendent of Documents, U.S. Government Printing Office, Washington, D.C. 20402. <input checked="" type="checkbox"/> Order From National Technical Information Service (NTIS), Springfield, VA. 22161		14. NO. OF PRINTED PAGES 58	15. Price \$10.00